High-Energy Resummation Effects in the Production of Mueller-Navelet Dijets at the LHC

Samuel Wallon

Université Pierre et Marie Curie

and

Laboratoire de Physique Théorique

CNRS / Université Paris Sud

Orsay

Heavy-Ions Meeting

IPhT

23 March 2016

D. Colferai, F. Schwennsen, L. Szymanowski, S. W., JHEP 1012 (2010) 026 [arXiv:1002.1365 [hep-ph]]

B. Ducloué, L. Szymanowski, S. W., JHEP 1305 (2013) 096 [arXiv:1302.7012 [hep-ph]]

B. Ducloué, L. Szymanowski, S. W., Phys. Rev. Lett. 112 (2014) 082003 [arXiv:1309.3229 [hep-ph]]

B. Ducloué, L. Szymanowski, S. W., Phys. Lett. B738 (2014) 311-316 [arXiv:1407.6593 [hep-ph]]

B. Ducloué, L. Szymanowski, S. W., Phys. Rev. D92 (2015) 7, 076002 [arXiv:1507.04735 [hep-ph]]

A. H. Mueller, L. Szymanowski, S. W., B.-W. Xiao, F. Yuan, JHEP 1603 (2016) 096 [arXiv:1512.07127 [hep-ph]]

R. Boussarie, B. Ducloué, L. Szymanowski, *in preparation*

Dealing wtih QCD is theoretically challenging

How to deal with QCD?

example: Compton scattering

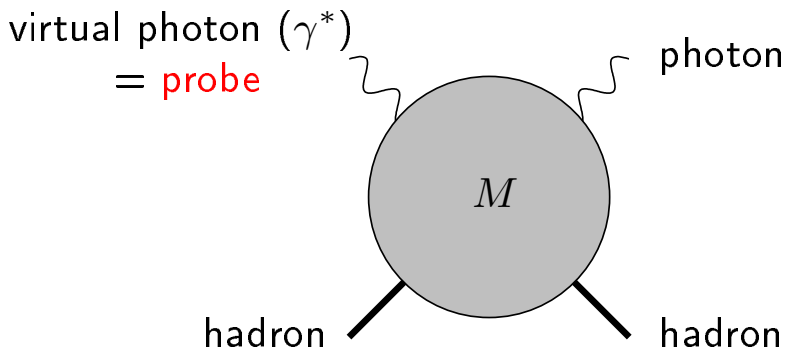

Aim: describe M by separating:

- quantities non-calculable perturbatively
  some tools:
  - Discretization of QCD on a 4-d lattice: numerical simulations
  - AdS/CFT $\Rightarrow$ AdS/QCD : $AdS_5 \times S^5 \leftrightarrow$ QCD
- pertubatively calculable quantities

Using perturbative QCD

Key question of QCD:
how to obtain and understand the tri-dimensional structure of hadrons in terms of quarks and gluons?

- The aim is to reduce the process to interactions involving a small number of *partons* (quarks, gluons), despite confinement

- This is possible if the considered process is driven by short distance phenomena ($d \ll 1\,\mathrm{fm}$)
  $\Longrightarrow \alpha_s \ll 1$: Perturbative methods
- One should hit strongly enough a hadron
  Example: electromagnetic probe and form factor

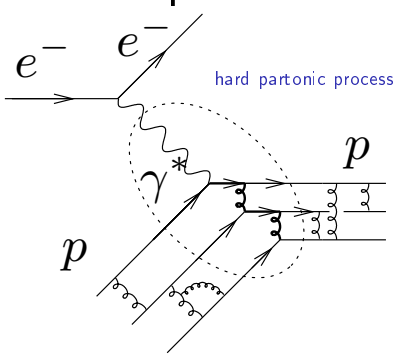

τ electromagnetic interaction $\sim \tau$ parton life time after interaction
$\ll \tau$ caracteristic time of strong interaction

To get such situations in exclusive reactions is very challenging phenomenologically: the cross sections are very small

Using perturbative QCD

Hard processes in QCD

- This is justified if the process is governed by a hard scale:
  - virtuality of the electromagnetic probe
    in elastic scattering $e^{\pm}\,p \to e^{\pm}\,p$
    in Deep Inelastic Scattering (DIS) $e^{\pm}\,p \to e^{\pm}\,X$
    in Deep Virtual Compton Scattering (DVCS) $e^{\pm}\,p \to e^{\pm}\,p\,\gamma$
  - Total center of mass energy in $e^+e^- \to X$ annihilation
  - t-channel momentum exchange in meson photoproduction $\gamma\,p \to M\,p$
- A precise treatment relies on factorization theorems
- The scattering amplitude is described by the convolution of the partonic amplitude with the non-perturbative hadronic content

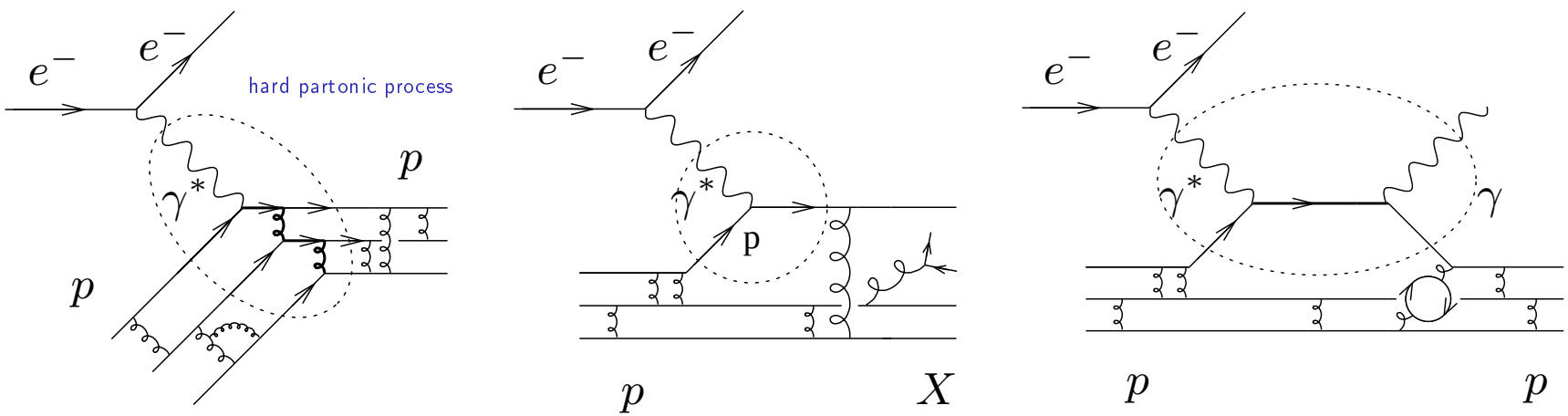

DIS

Accessing the perturbative proton content using inclusive processes

no $1/Q$ suppression

example: DIS

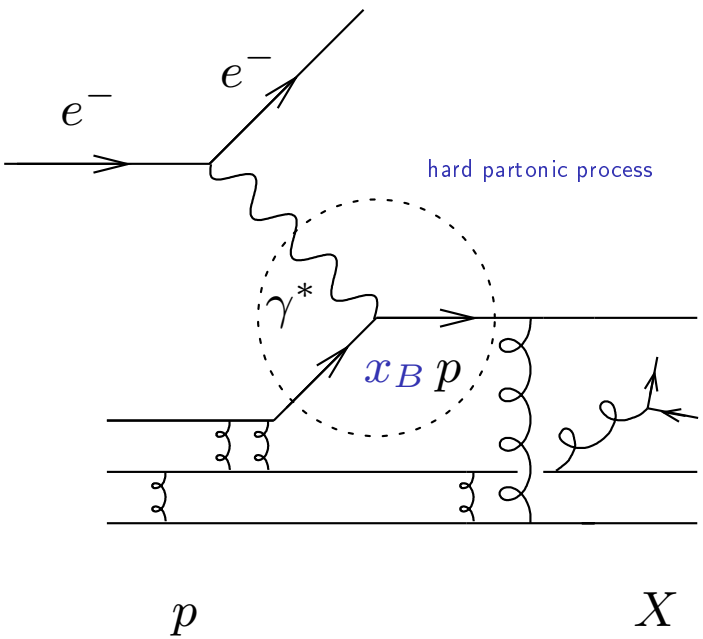

$$s_{\gamma^* p} = (q_\gamma^* + p_p)^2 = 4\, E^2_{\text{c.m.}}$$

$$Q^2 \equiv -q^2_{\gamma^*} > 0$$

$$x_B = \frac{Q^2}{2\, p_p \cdot q_\gamma^*} \simeq \frac{Q^2}{s_{\gamma^* p}}$$

- x_B = proton momentum fraction carried by the scattered quark
- $1/Q$ = transverse resolution of the photonic probe $\ll 1/\Lambda_{QCD}$

DIS

The various regimes governing the perturbative content of the proton

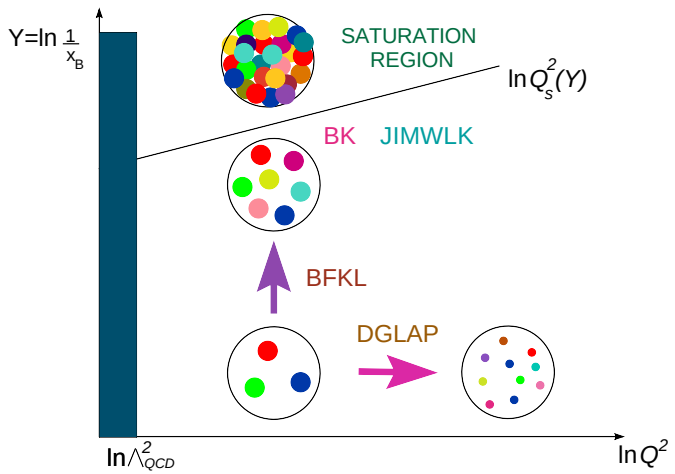

- "usual" regime: x_B moderate ($x_B \gtrsim .01$):
  Evolution in Q governed by the QCD renormalization group
  (Dokshitser, Gribov, Lipatov, Altarelli, Parisi equation)

$$\underbrace{\sum_n (\alpha_s \ln Q^2)^n}_{\text{LLQ}} + \alpha_s \underbrace{\sum_n (\alpha_s \ln Q^2)^n}_{\text{NLLQ}} + \cdots$$

- perturbative Regge limit: $s_{\gamma^* p} \to \infty$ i.e. $x_B \sim Q^2/s_{\gamma^* p} \to 0$
  in the perturbative regime (hard scale Q^2)
  (Balitski Fadin Kuraev Lipatov equation)

$$\underbrace{\sum_n (\alpha_s \ln s)^n}_{\text{LLs}} + \alpha_s \underbrace{\sum_n (\alpha_s \ln s)^n}_{\text{NLLs}} + \cdots$$

QCD in the perturbative Regge limit

- One of the important longstanding theoretical questions raised by QCD is its behaviour in the perturbative Regge limit $s \gg -t$
- Based on theoretical grounds, one should identify and test suitable observables in order to test this peculiar dynamics

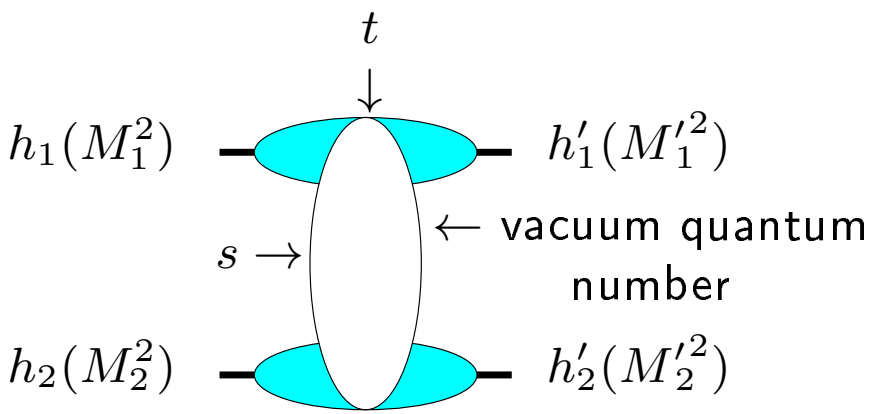

hard scales: $M_1^2,\ M_2^2 \gg \Lambda_{QCD}^2$ or $M_1'^2,\ M_2'^2 \gg \Lambda_{QCD}^2$ or $t \gg \Lambda_{QCD}^2$
where the $t-$channel exchanged state is the so-called hard Pomeron

How to test QCD in the perturbative Regge limit?

What kind of observable?

- perturbation theory should be applicable:
  selecting external or internal probes with transverse sizes $\ll 1/\Lambda_{QCD}$ (*hard* γ^*, *heavy* meson (J/Ψ, Υ), *energetic* forward jets) or by choosing large t in order to provide the hard scale.

- governed by the *"soft"* perturbative dynamics of QCD

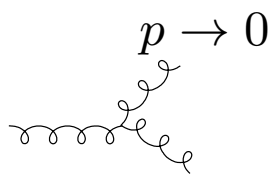

  and *not* by its *collinear* dynamics

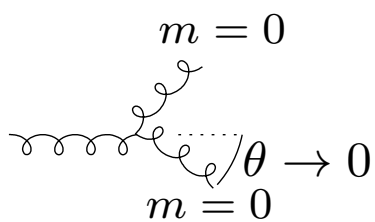

  $\Longrightarrow$ select semi-hard processes with $s \gg p_{T\,i}^2 \gg \Lambda_{QCD}^2$ where $p_{T\,i}^2$ are typical transverse scale, all of the same order.

How to test QCD in the perturbative Regge limit?

Some examples of processes

- inclusive: DIS (HERA), diffractive DIS, total $\gamma^*\gamma^*$ cross-section (LEP, ILC)
- semi-inclusive: forward jet and π^0 production in DIS, Mueller-Navelet double jets, diffractive double jets, high p_T central jet, in hadron-hadron colliders (Tevatron, LHC)
- exclusive: exclusive meson production in DIS, double diffractive meson production at e^+e^- colliders (ILC), ultraperipheral events at LHC ($\mathbb{P}$omeron, $\mathbb{O}$dderon)

Resummation in QCD: DGLAP vs BFKL

Small values of α_s (perturbation theory applies if there is a hard scale) can be compensated by large logarithmic enhancements.

DGLAP

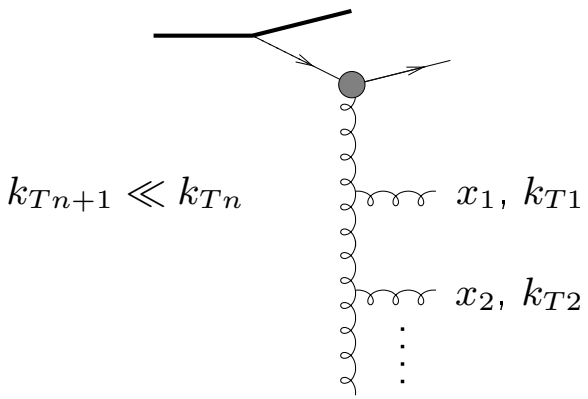

strong ordering in k_T

$$\sum(\alpha_s \ln Q^2)^n$$

BFKL

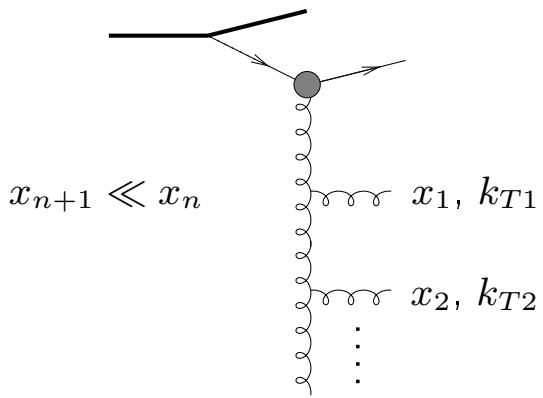

strong ordering in x

$$\sum(\alpha_s \ln s)^n$$

When $\sqrt{s}$ becomes very large, it is expected that a BFKL description is needed to get accurate predictions

The specific case of QCD at large s

QCD in the perturbative Regge limit

The amplitude can be written as:

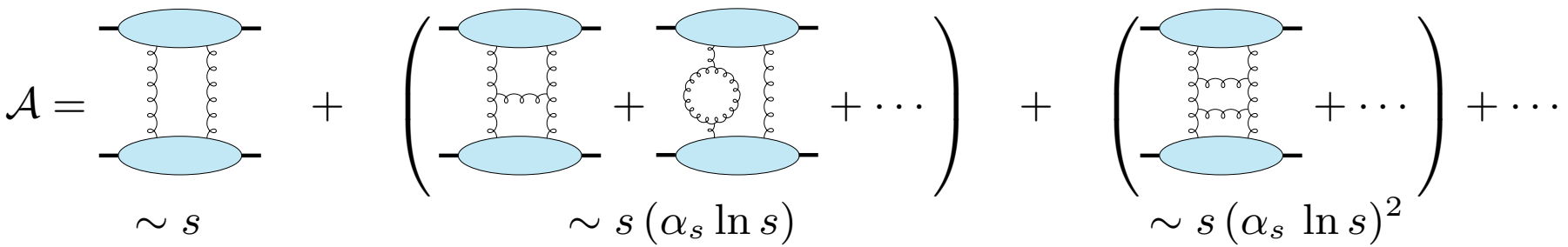

this can be put in the following form :

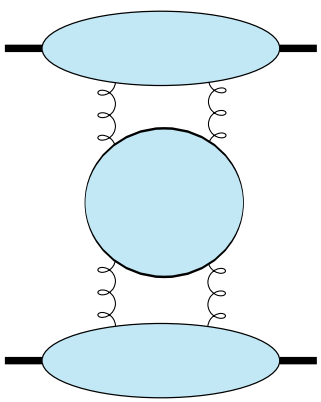

← Impact factor

← Green's function

← Impact factor

$$\sigma_{tot}^{h_1\,h_2 \to anything} = \frac{1}{s} Im\mathcal{A} \sim s^{\alpha_{\mathbb{P}}(0)-1}$$

with $\alpha_{\mathbb{P}}(0) - 1 = C\,\alpha_s + C'\,\alpha_s^2 + \cdots$

$C > 0$: Leading Log $\mathbb{P}$omeron

Balitsky, Fadin, Kuraev, Lipatov

Opening the boxes: Impact representation $\gamma^*\,\gamma^* \to \gamma^*\,\gamma^*$ as an example

- Sudakov decomposition: $k_i = \alpha_i\, p_1 + \beta_i\, p_2 + k_{\perp i} \quad (p_1^2 = p_2^2 = 0,\ 2p_1 \cdot p_2 = s)$
- write $d^4k_i = \frac{s}{2}\, d\alpha_i\, d\beta_i\, d^2k_{\perp i} \qquad (\underline{k} = \text{Eucl.} \leftrightarrow k_\perp = \text{Mink.})$
- $t-$channel gluons have non-sense polarizations at large s: $\epsilon_{NS}^{up/down} = \frac{2}{s}\, p_{2/1}$

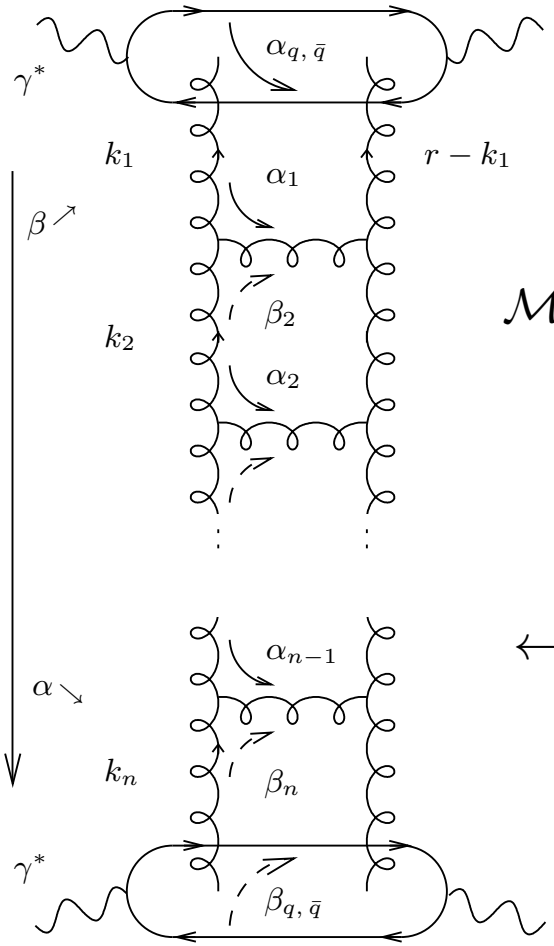

$\Rightarrow$ set $\alpha_1 = 0$ and $\int d\beta_1$ $\Rightarrow$ $\Phi^{\gamma^*\to\gamma^*}(\underline{k}_1, \underline{r} - \underline{k}_1)$
impact factor

$$\mathcal{M} = \frac{is}{(2\pi)^2}\int \frac{d^2\underline{k}}{\underline{k}^2}\,\Phi^{up}(\underline{k},\,\underline{r}-\underline{k})\int \frac{d^2\underline{k}'}{\underline{k}'^2}\,\Phi^{down}(-\underline{k}',\,-\underline{r}+\underline{k}') \times \int_{\delta-i\infty}^{\delta+i\infty}\frac{d\omega}{2\pi i}\left(\frac{s}{s_0}\right)^{\omega} G_\omega(\underline{k},\underline{k}',\underline{r})$$

$\longleftarrow$ multi-Regge kinematics

$\Rightarrow$ set $\beta_n = 0$ and $\int d\alpha_n$ $\Rightarrow$ $\Phi^{\gamma^*\to\gamma^*}(-\underline{k}_n, -\underline{r} + \underline{k}_n)$

Higher order corrections

- Higher order corrections to BFKL kernel are known at NLL order (Lipatov Fadin; Camici, Ciafaloni), now for arbitrary impact parameter $\alpha_S \sum_n (\alpha_S \ln s)^n$ resummation

- impact factors are known in some cases at NLL
  - $\gamma^* \to \gamma^*$ at $t = 0$ (Bartels, Colferai, Gieseke, Kyrieleis, Qiao; Balitski, Chirilli)
  - forward jet production (Bartels, Colferai, Vacca; Caporale, Ivanov, Murdaca, Papa, Perri; Chachamis, Hentschinski, Madrigal, Sabio Vera)
  - inclusive production of a pair of hadrons separated by a large interval of rapidity (Ivanov, Papa)
  - $\gamma^*_L \to \rho_L$ in the forward limit (Ivanov, Kotsky, Papa)

Mueller-Navelet jets: Basics

Mueller-Navelet jets

- Consider two jets (hadrons flying within a narrow cone) separated by a large rapidity, i.e. each of them almost fly in the direction of the hadron "close" to it, and with very similar transverse momenta
- Pure LO *collinear* treatment: these two jets should be emitted back to back at leading order:
  - $\varphi \equiv \Delta\phi - \pi = 0$ ($\Delta\phi = \phi_1 - \phi_2$ = relative azimuthal angle)
  - $k_{\perp 1}$=$k_{\perp 2}$. No phase space for (untagged) multiple (DGLAP) emission between them

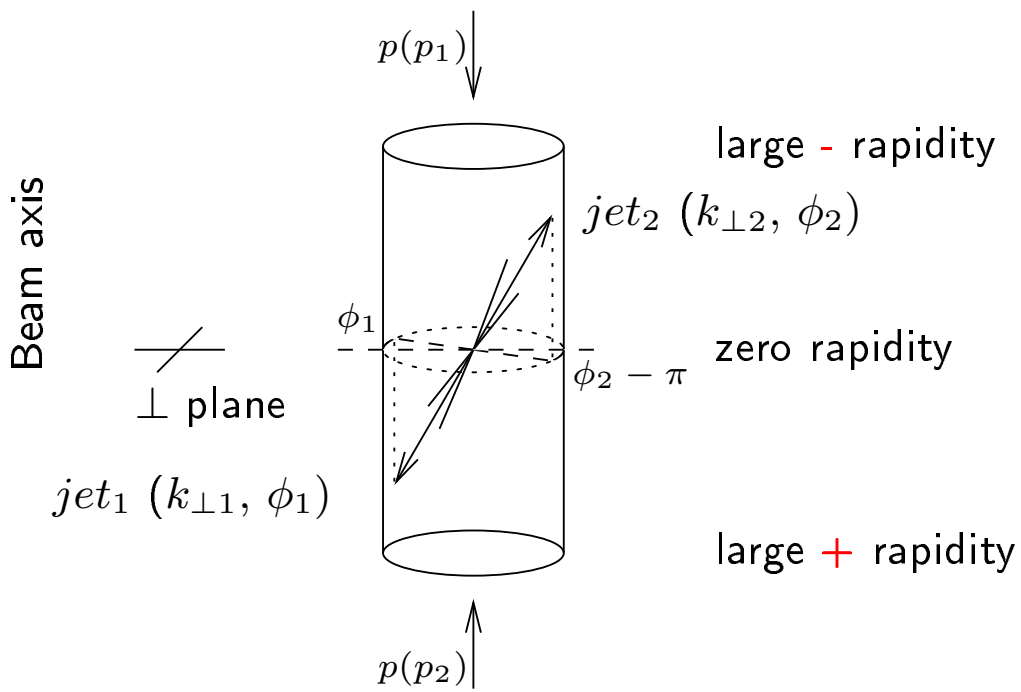

Mueller-Navelet jets at LL fails

Mueller Navelet jets at LL BFKL

- in LL BFKL ($\sim \sum (\alpha_s \ln s)^n$), emission between these jets $\longrightarrow$ strong decorrelation between the relative azimutal angle jets, incompatible with $p\bar{p}$ Tevatron collider data
- a collinear treatment at next-to-leading order (NLO) can describe the data
- important issue: non-conservation of energy-momentum along the BFKL ladder. A LL BFKL-based Monte Carlo combined with e-m conservation improves dramatically the situation (Orr and Stirling)

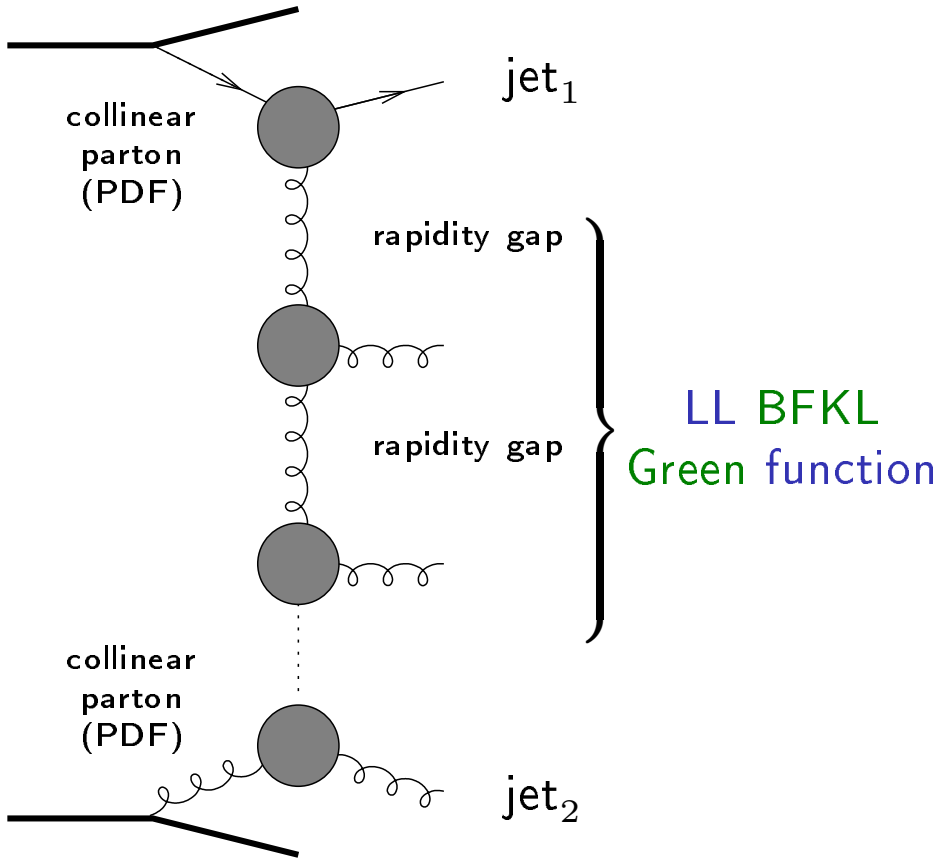

Multi-Regge kinematics (LL BFKL)

Studies at LHC: Mueller-Navelet jets

Mueller Navelet jets at NLL BFKL

- up to now, the subseries $\alpha_s \sum (\alpha_s \ln s)^n$ NLL was included only in the exchanged $\mathbb{P}$omeron state, and not inside the jet vertices
  Sabio Vera, Schwennsen
  Marquet, Royon
- the common belief was that these corrections should not be important

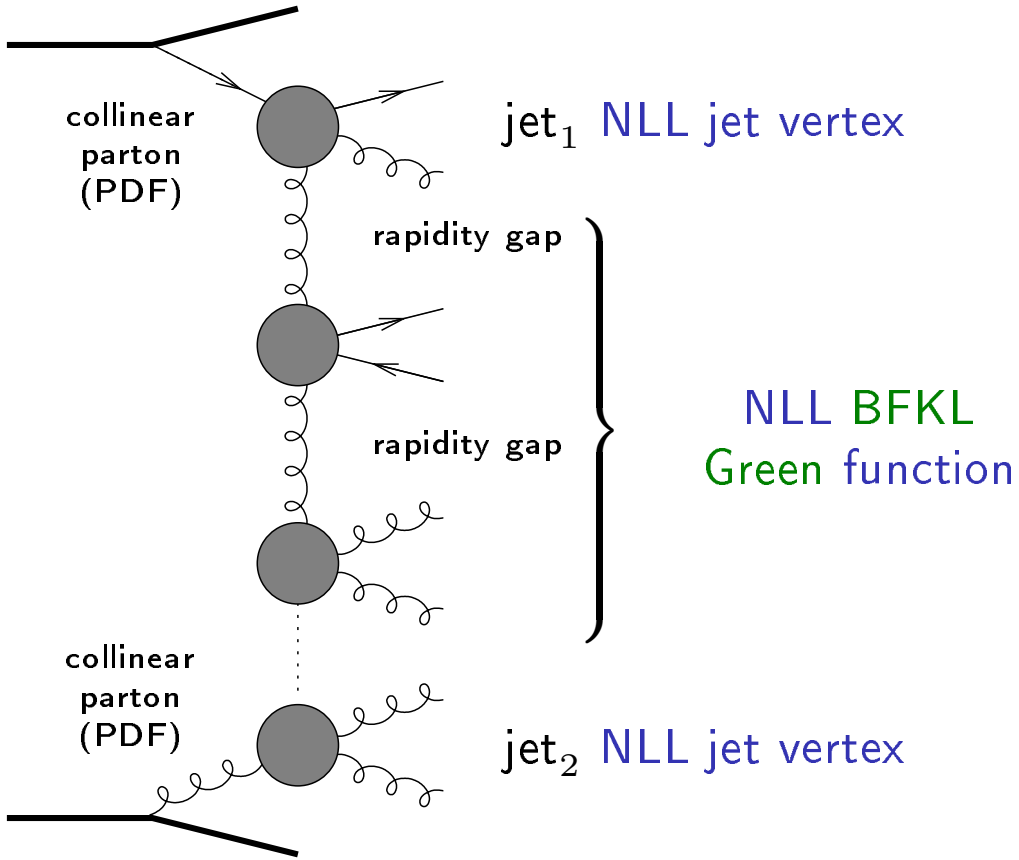

Quasi Multi-Regge kinematics (here for NLL BFKL)

Master formulas

k_T-factorized differential cross section

$$\frac{\mathrm{d}\sigma}{\mathrm{d}|\mathbf{k}_{J1}|\,\mathrm{d}|\mathbf{k}_{J2}|\,\mathrm{d}y_{J1}\,\mathrm{d}y_{J2}} = \int \mathrm{d}\phi_{J1}\,\mathrm{d}\phi_{J2} \int \mathrm{d}^2\mathbf{k}_1\,\mathrm{d}^2\mathbf{k}_2$$

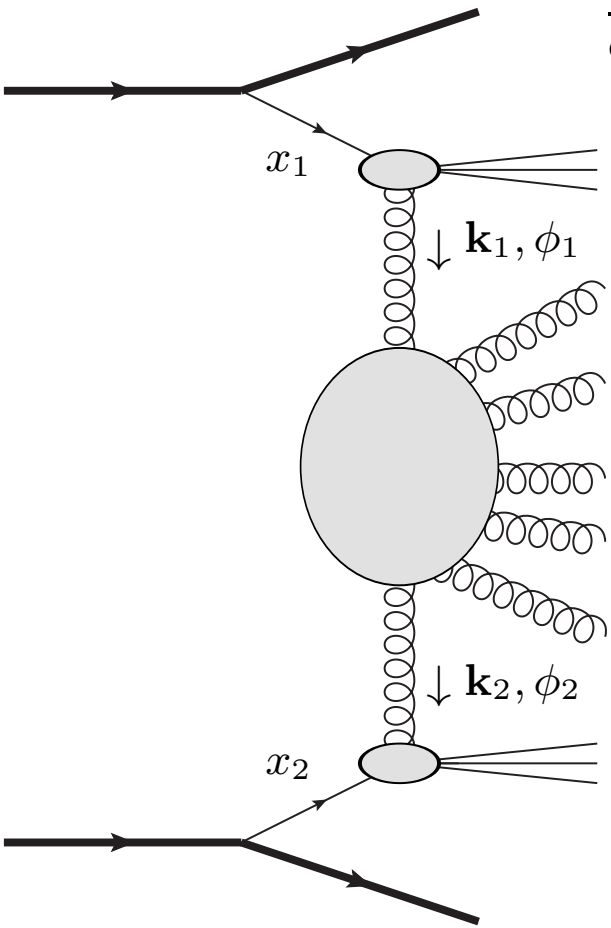

$$\times \Phi(\mathbf{k}_{J1}, x_{J1}, -\mathbf{k}_1)$$

$$\times G(\mathbf{k}_1, \mathbf{k}_2, \hat{s})$$

$$\times \Phi(\mathbf{k}_{J2}, x_{J2}, \mathbf{k}_2)$$

with $\Phi(\mathbf{k}_{J2}, x_{J2}, \mathbf{k}_2) = \int \mathrm{d}x_2\, f(x_2) V(\mathbf{k}_2, x_2)$ $\quad f \equiv$ PDF $\quad x_J = \frac{|\mathbf{k}_J|}{\sqrt{s}} e^{y_J}$

Results

Results for a symmetric configuration

In the following we show results for

- $\sqrt{s} = 7$ TeV
- $35\,\mathrm{GeV} < |\mathbf{k}_{J1}|\,, |\mathbf{k}_{J2}| < 60\,\mathrm{GeV}$
- $0 < |y_1|\,, |y_2| < 4.7$

These cuts allow us to compare our predictions with the first experimental data on azimuthal correlations of Mueller-Navelet jets at the LHC presented by the CMS collaboration (CMS-PAS-FSQ-12-002) and submitted a two months ago (1601.06713 [hep-ex])

note: unlike experiments we have to set an upper cut on $|\mathbf{k}_{J1}|$ and $|\mathbf{k}_{J2}|$. We have checked that our results do not depend on this cut significantly.

Results: azimuthal correlations

Azimuthal correlation $\langle \cos\varphi \rangle$

$$\frac{\mathcal{C}_1}{\mathcal{C}_0} = \langle \cos\varphi \rangle \equiv \langle \cos(\phi_{J1} - \phi_{J2} - \pi) \rangle$$

recall: $\varphi = 0 \Leftrightarrow$ back-to-back

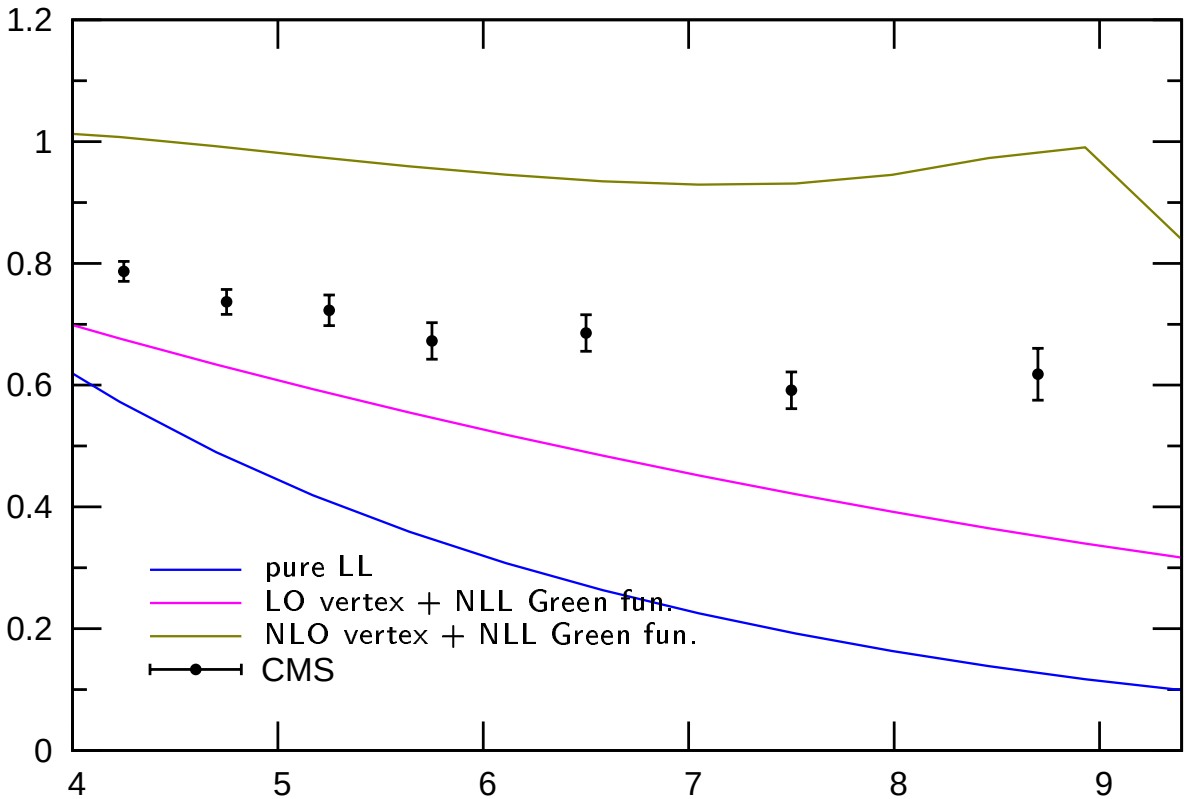

$$35\,\text{GeV} < |\mathbf{k}_{J1}| < 60\,\text{GeV}$$
$$35\,\text{GeV} < |\mathbf{k}_{J2}| < 60\,\text{GeV}$$

$$0 < |y_1| < 4.7$$
$$0 < |y_2| < 4.7$$

$$Y \equiv |y_1 - y_2|$$

The NLO corrections to the jet vertex lead to a large increase of the correlation

Note: LO vertex + NLL Green done by F. Schwennsen, A. Sabio-Vera; C. Marquet, C. Royon

Results: azimuthal correlations

Azimuthal correlation $\langle \cos\varphi \rangle$

$$\langle \cos\varphi \rangle \equiv \langle \cos(\phi_{J1} - \phi_{J2} - \pi) \rangle$$

recall: $\varphi = 0 \Leftrightarrow$ back-to-back

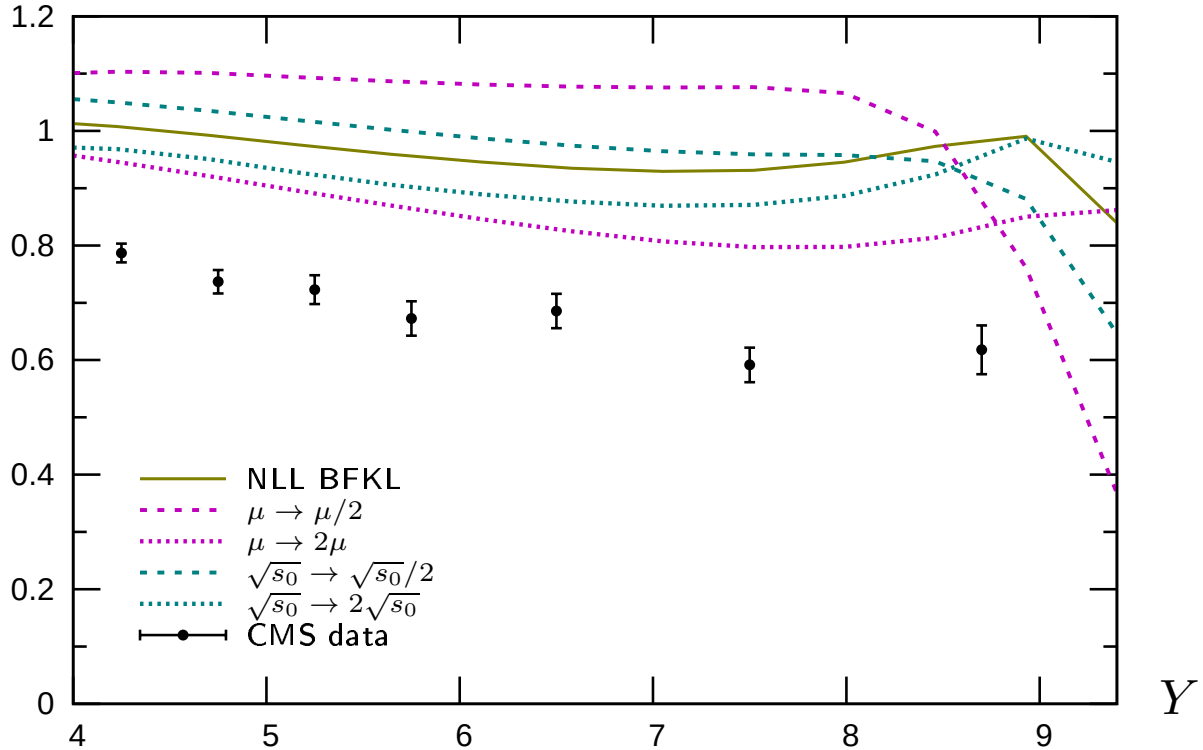

$$35\,\text{GeV} < |\mathbf{k}_{J1}| < 60\,\text{GeV}$$
$$35\,\text{GeV} < |\mathbf{k}_{J2}| < 60\,\text{GeV}$$

$$0 < |y_1| < 4.7$$
$$0 < |y_2| < 4.7$$

- NLL BFKL predicts a too small decorrelation
- The NLL BFKL calculation is still rather dependent on the scales, especially the renormalization / factorization scale

Results: azimuthal correlations

Azimuthal correlation $\langle \cos 2\varphi \rangle$

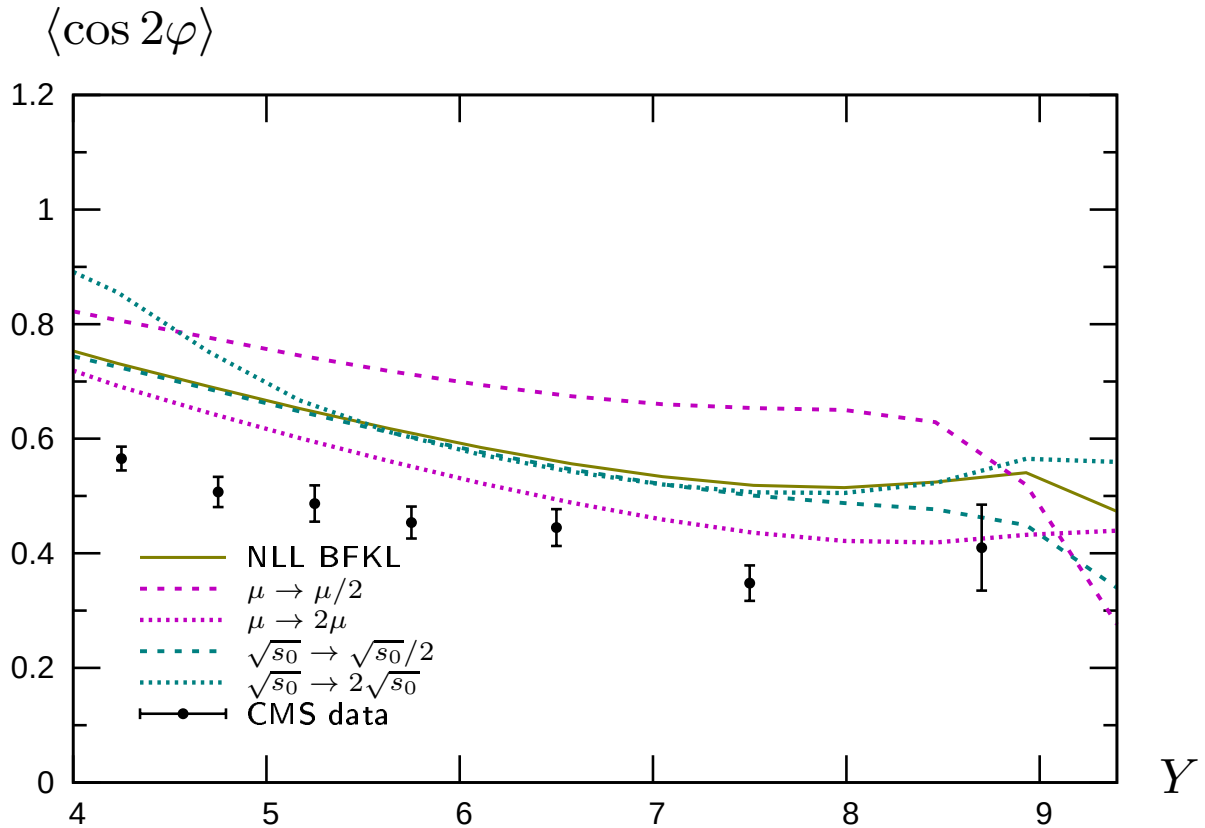

recall: $\varphi = 0 \Leftrightarrow$ back-to-back

$$35\,\text{GeV} < |\mathbf{k}_{J1}| < 60\,\text{GeV}$$
$$35\,\text{GeV} < |\mathbf{k}_{J2}| < 60\,\text{GeV}$$

$$0 < |y_1| < 4.7$$
$$0 < |y_2| < 4.7$$

- The agreement with data is a little better for $\langle \cos 2\varphi \rangle$ but still not very good
- This observable is also very sensitive to the scales

Results: azimuthal correlations

Azimuthal correlation $\langle \cos 2\varphi \rangle / \langle \cos \varphi \rangle$

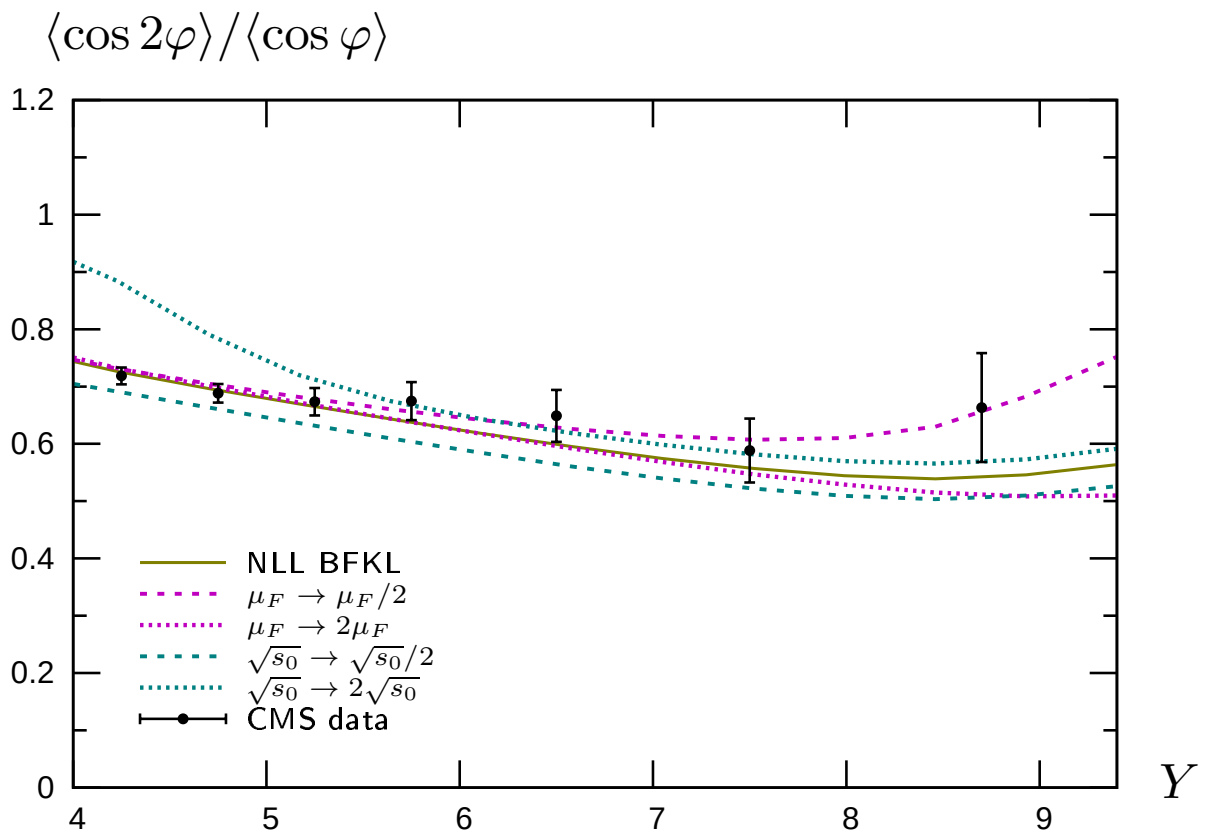

recall: $\varphi = 0 \Leftrightarrow$ back-to-back

$$35\,\text{GeV} < |\mathbf{k}_{J1}| < 60\,\text{GeV}$$
$$35\,\text{GeV} < |\mathbf{k}_{J2}| < 60\,\text{GeV}$$

$$0 < |y_1| < 4.7$$
$$0 < |y_2| < 4.7$$

- This observable is more stable with respect to the scales than the previous ones
- The agreement with data is good across the whole Y range

Results: azimuthal correlations

Azimuthal correlation $\langle \cos 2\varphi \rangle / \langle \cos \varphi \rangle$

$\langle \cos 2\varphi \rangle / \langle \cos \varphi \rangle$

recall: $\varphi = 0 \Leftrightarrow$ back-to-back

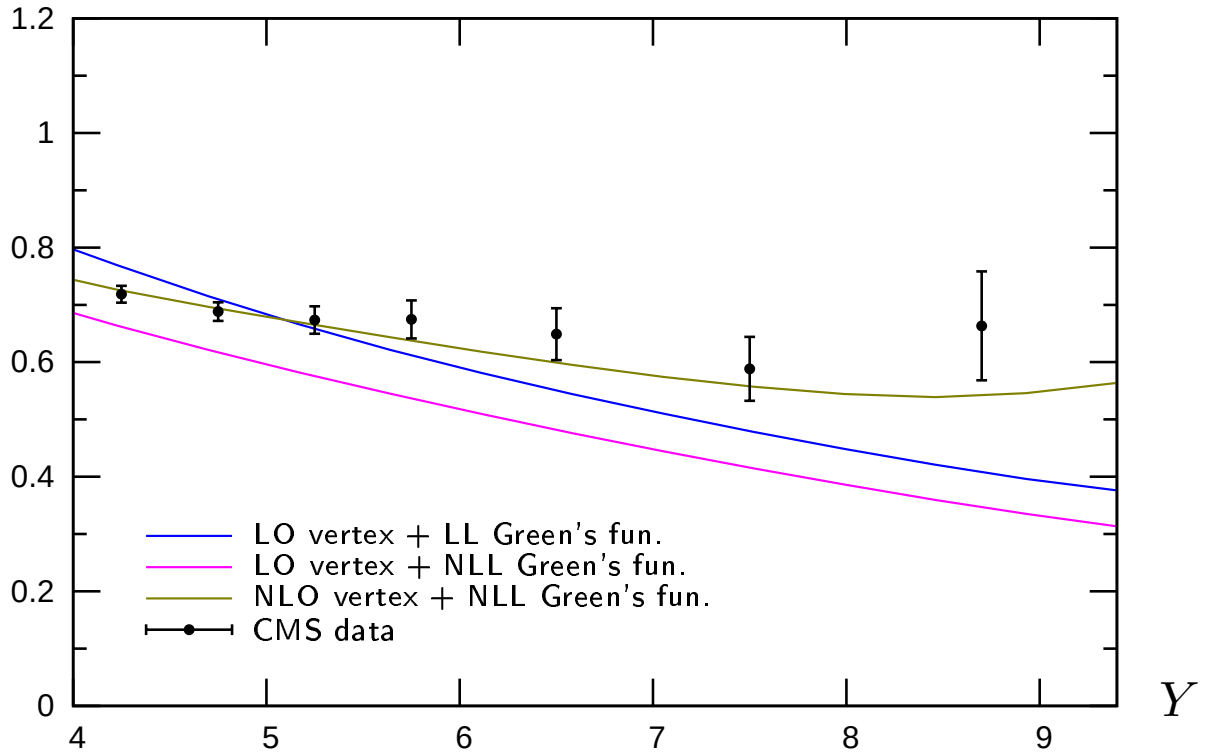

$35\,\mathrm{GeV} < |\mathbf{k}_{J1}| < 60\,\mathrm{GeV}$

$35\,\mathrm{GeV} < |\mathbf{k}_{J2}| < 60\,\mathrm{GeV}$

$0 < |y_1| < 4.7$

$0 < |y_2| < 4.7$

It is necessary to include the NLO corrections to the jet vertex to reproduce the behavior of the data at large Y

Results: azimuthal distribution

Azimuthal distribution (integrated over $6 < Y < 9.4$)

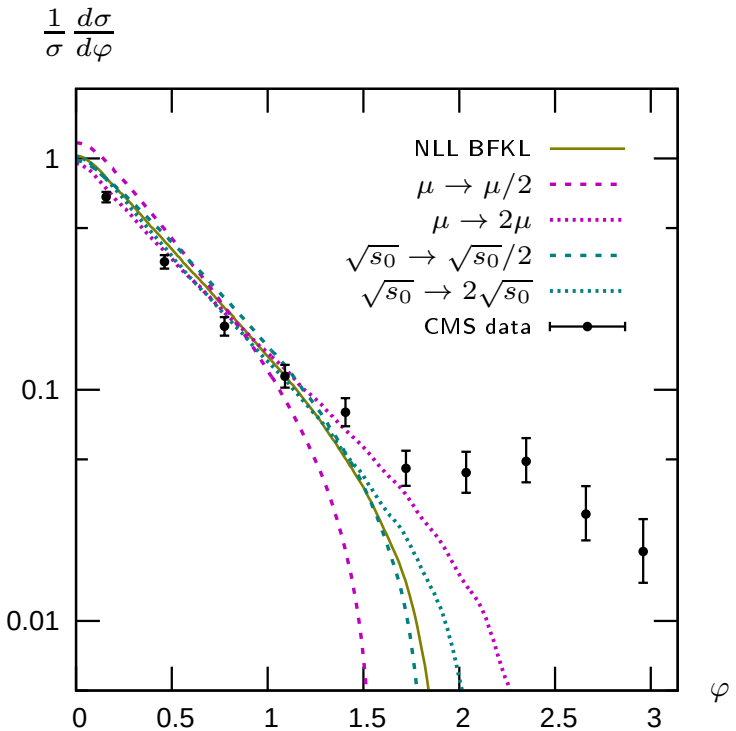

recall: $\varphi = 0 \Leftrightarrow$ back-to-back

$$\frac{1}{\sigma}\frac{d\sigma}{d\varphi} = \frac{1}{2\pi}\left\{1 + 2\sum_{n=1}^{\infty}\cos\left(n\varphi\right)\left\langle\cos\left(n\varphi\right)\right\rangle\right\}.$$

- Our calculation predicts a too large value of $\frac{1}{\sigma}\frac{d\sigma}{d\varphi}$ for $\varphi \lesssim \frac{\pi}{2}$ and a too small value for $\varphi \gtrsim \frac{\pi}{2}$
- It is not possible to describe the data even when varying the scales by a factor of 2

Results: limitations

- The agreement of our calculation with the data for $\langle \cos 2\varphi \rangle / \langle \cos \varphi \rangle$ is good and quite stable with respect to the scales
- The agreement for $\langle \cos n\varphi \rangle$ and $\frac{1}{\sigma}\frac{d\sigma}{d\varphi}$ is not very good and very sensitive to the choice of the renormalization scale μ_R
- An all-order calculation would be independent of the choice of μ_R. This feature is lost if we truncate the perturbative series
  $\Rightarrow$ How to choose the renormalization scale?
  'Natural scale': sometimes the typical momenta in a loop diagram are different from the natural scale of the process

We decided to use the Brodsky-Lepage-Mackenzie (BLM) procedure to fix the renormalization scale

The BLM renormalization scale fixing procedure

The Brodsky-Lepage-Mackenzie (BLM) procedure resums the self-energy corrections to the gluon propagator at one loop into the running coupling.

First attempts to apply BLM scale fixing to BFKL processes lead to problematic results. Brodsky, Fadin, Kim, Lipatov and Pivovarov suggested that one should first go to a physical renormalization scheme like MOM and then apply the 'traditional' BLM procedure, i.e. identify the β_0 dependent part and choose μ_R such that it vanishes.

We followed this prescription for the full amplitude at NLL.

Results with BLM

Azimuthal correlation $\langle \cos \varphi \rangle$

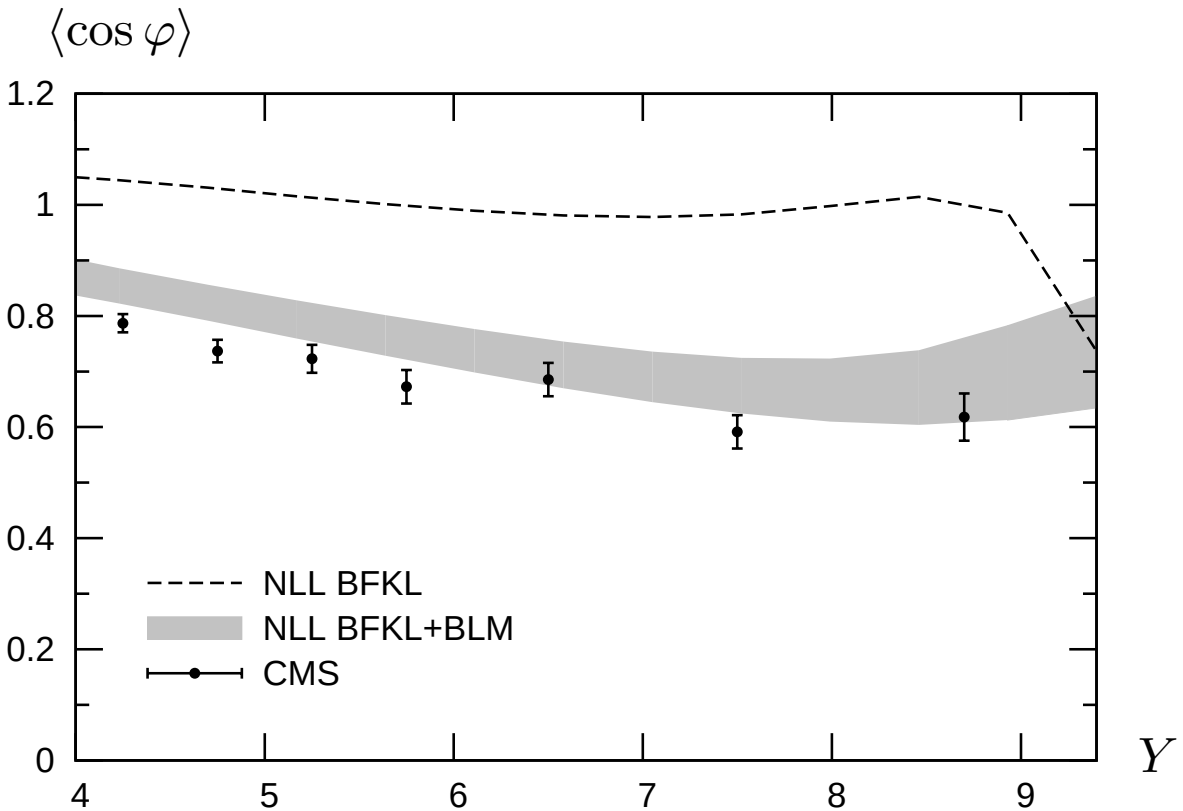

$$35\,\text{GeV} < |\mathbf{k}_{J1}| < 60\,\text{GeV}$$
$$35\,\text{GeV} < |\mathbf{k}_{J2}| < 60\,\text{GeV}$$

$$0 < |y_1| < 4.7$$
$$0 < |y_2| < 4.7$$

Using the BLM scale setting, the agreement with data becomes much better

Results with BLM

Azimuthal correlation $\langle \cos 2\varphi \rangle$

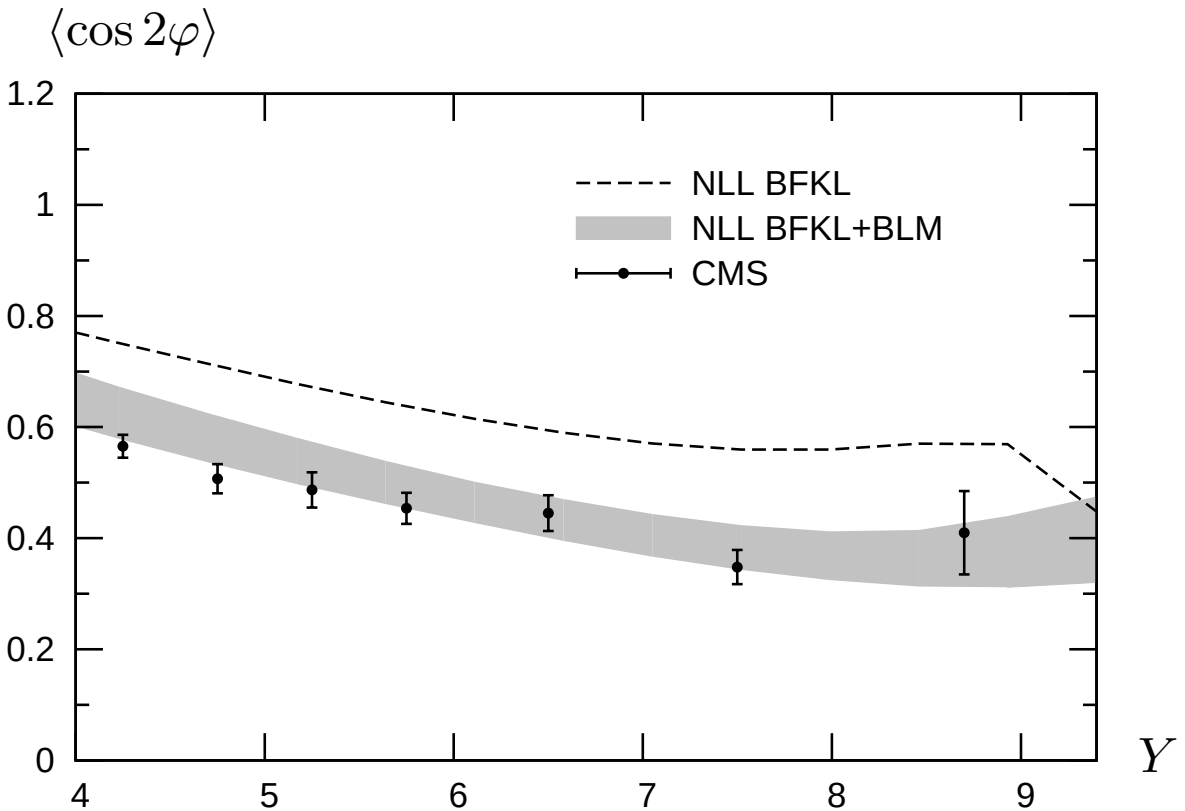

$35\,\mathrm{GeV} < |\mathbf{k}_{J1}| < 60\,\mathrm{GeV}$

$35\,\mathrm{GeV} < |\mathbf{k}_{J2}| < 60\,\mathrm{GeV}$

$0 < |y_1| < 4.7$

$0 < |y_2| < 4.7$

Using the BLM scale setting, the agreement with data becomes much better.

Results with BLM

Azimuthal correlation $\langle \cos 2\varphi \rangle / \langle \cos \varphi \rangle$

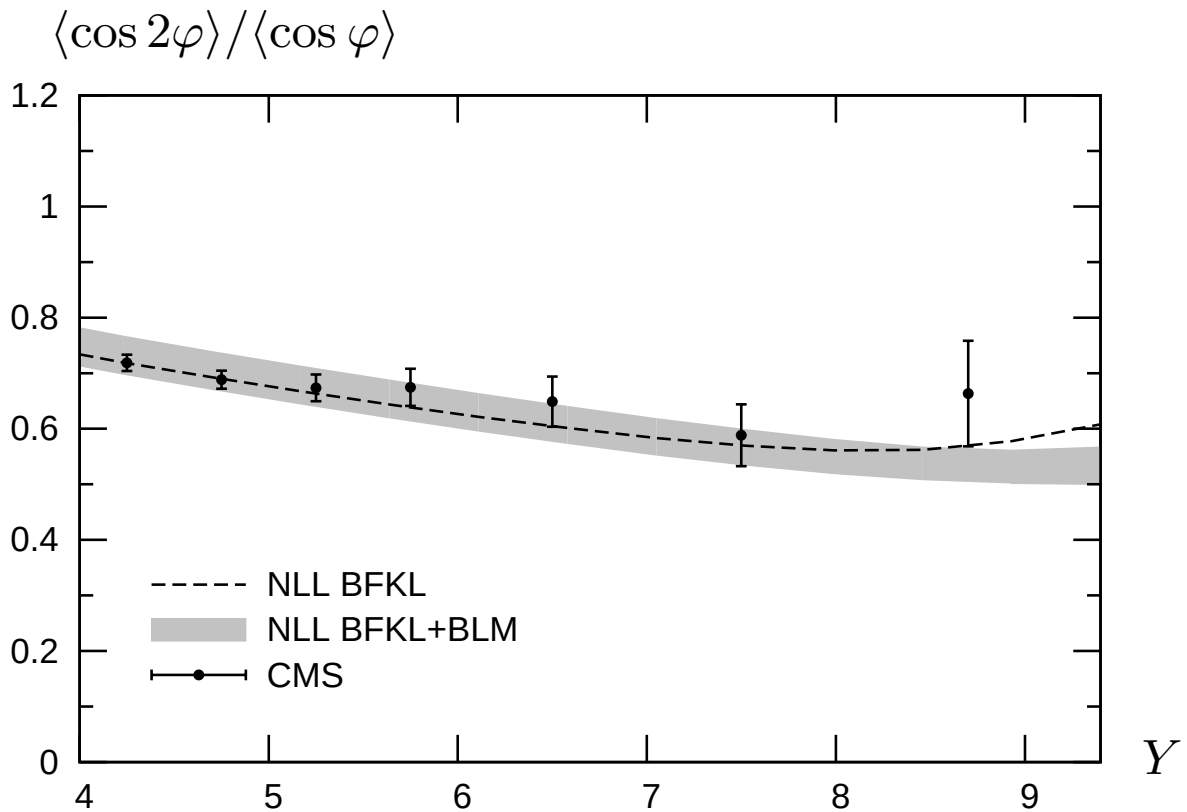

$35\,\mathrm{GeV} < |\mathbf{k}_{J1}| < 60\,\mathrm{GeV}$

$35\,\mathrm{GeV} < |\mathbf{k}_{J2}| < 60\,\mathrm{GeV}$

$0 < |y_1| < 4.7$

$0 < |y_2| < 4.7$

Because it is much less dependent on the scales, the observable $\langle \cos 2\varphi \rangle / \langle \cos \varphi \rangle$ is almost not affected by the BLM procedure and is still in good agreement with the data.

Results with BLM

Azimuthal distribution (integrated over $6 < Y < 9.4$)

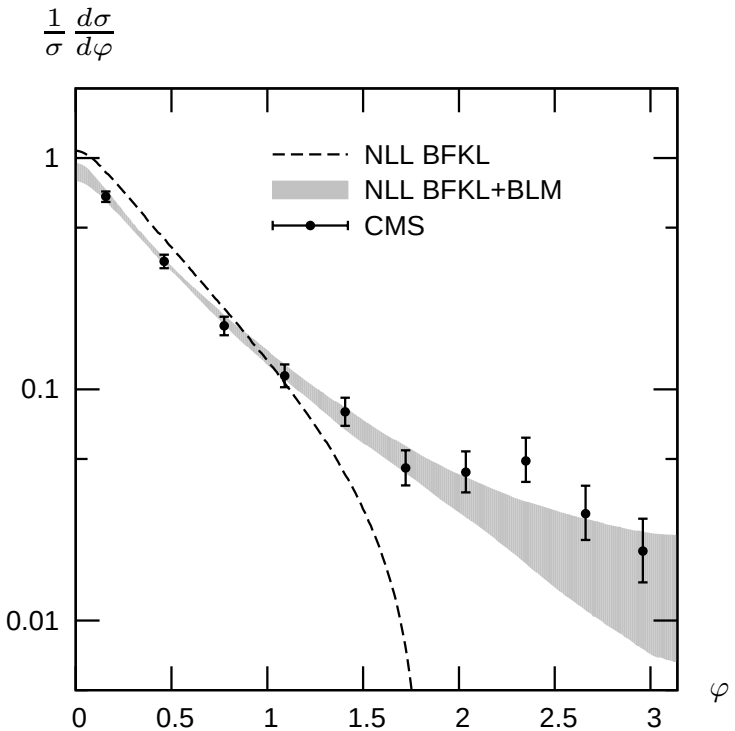

With the BLM scale setting the azimuthal distribution is in good agreement with the data across the full φ range.

Comparison with fixed-order

Using the BLM scale setting:

- The agreement $\langle \cos n\varphi \rangle$ with the data becomes much better
- The agreement for $\langle \cos 2\varphi \rangle / \langle \cos \varphi \rangle$ is still good and unchanged as this observable is weakly dependent on μ_R
- The azimuthal distribution is in much better agreement with the data

But the configuration chosen by CMS with $|\mathbf{k}_{J1}|_{\min} = |\mathbf{k}_{J2}|_{\min}$ does not allow us to compare with a fixed-order $\mathcal{O}(\alpha_s^3)$ treatment (i.e. without resummation)

- These calculations are unstable when $|\mathbf{k}_{J1}|_{\min} = |\mathbf{k}_{J2}|_{\min}$ because the cancellation of some IR divergencies is difficult to obtain numerically
- Resummation effects à la Sudakov are important in the limit $\mathbf{k}_{J1} \simeq -\mathbf{k}_{J2}$ and require a special treatment.
  - This resummation has been obtained at LL
    A. H. Mueller, L. Szymanowski, S. W., B.-W. Xiao, F. Yuan, arXiv:1512.07127 [hep-ph]
  - The evaluation of the magnitude of this effect remains to be done
  - Beyond LL, it is presumably very tricky ...
- This resummation is not available in fixed-order treatments

Comparison with fixed-order

Results for an asymmetric configuration

In this section we choose the cuts as

- $35\,\mathrm{GeV} < |\mathbf{k}_{J1}|\,, |\mathbf{k}_{J2}| < 60\,\mathrm{GeV}$
- $50\,\mathrm{GeV} < \mathrm{Max}(|\mathbf{k}_{J1}|, |\mathbf{k}_{J2}|)$
- $0 < |y_1|\,, |y_2| < 4.7$

and we compare our results with the NLO fixed-order code Dijet (Aurenche, Basu, Fontannaz) in the same configuration

Comparison with fixed-order

Azimuthal correlation $\langle \cos \varphi \rangle$

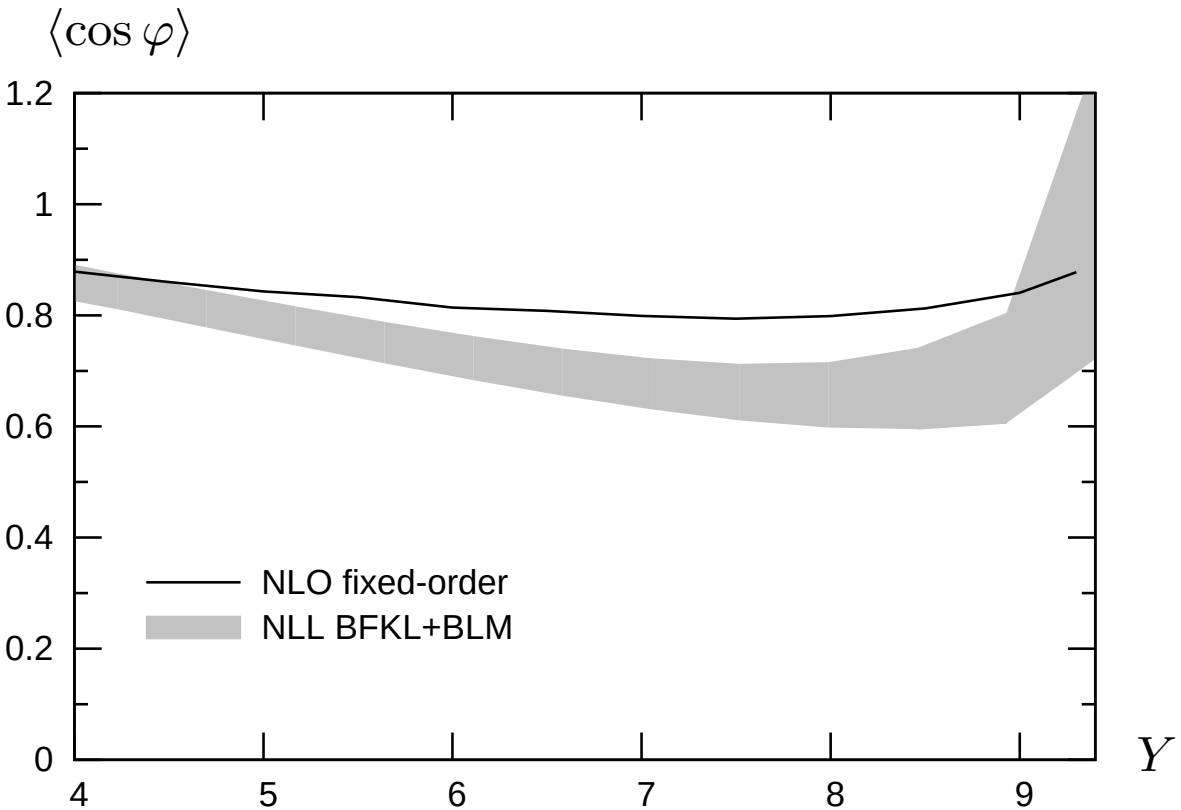

$$35\,\mathrm{GeV} < |\mathbf{k}_{J1}| < 60\,\mathrm{GeV}$$
$$35\,\mathrm{GeV} < |\mathbf{k}_{J2}| < 60\,\mathrm{GeV}$$
$$50\,\mathrm{GeV} < \mathrm{Max}(|\mathbf{k}_{J1}|, |\mathbf{k}_{J2}|)$$

$$0 < |y_1| < 4.7$$
$$0 < |y_2| < 4.7$$

The NLO fixed-order and NLL BFKL+BLM calculations are very close

Comparison with fixed-order

Azimuthal correlation $\langle \cos 2\varphi \rangle$

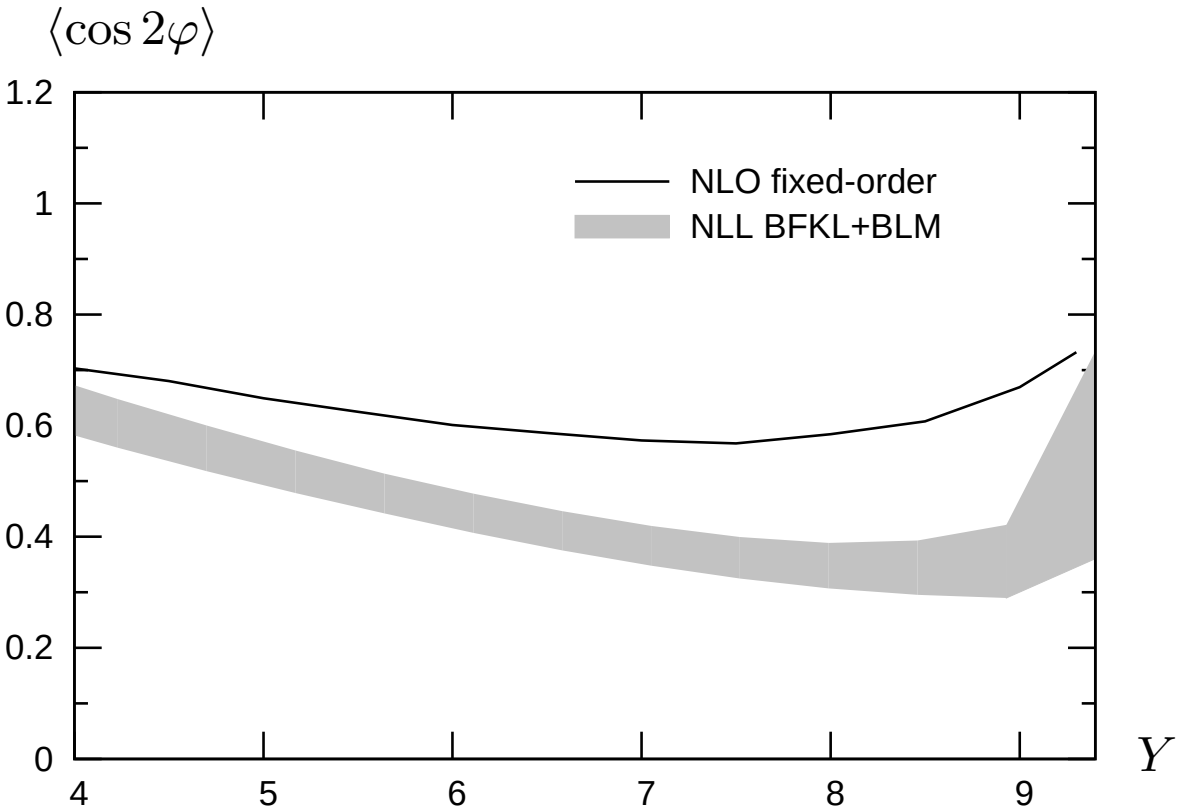

$$35\,\text{GeV} < |\mathbf{k}_{J1}| < 60\,\text{GeV}$$
$$35\,\text{GeV} < |\mathbf{k}_{J2}| < 60\,\text{GeV}$$
$$50\,\text{GeV} < \text{Max}(|\mathbf{k}_{J1}|, |\mathbf{k}_{J2}|)$$

$$0 < |y_1| < 4.7$$
$$0 < |y_2| < 4.7$$

The BLM procedure leads to a sizable difference between NLO fixed-order and NLL BFKL+BLM.

Comparison with fixed-order

Azimuthal correlation $\langle \cos 2\varphi \rangle / \langle \cos \varphi \rangle$

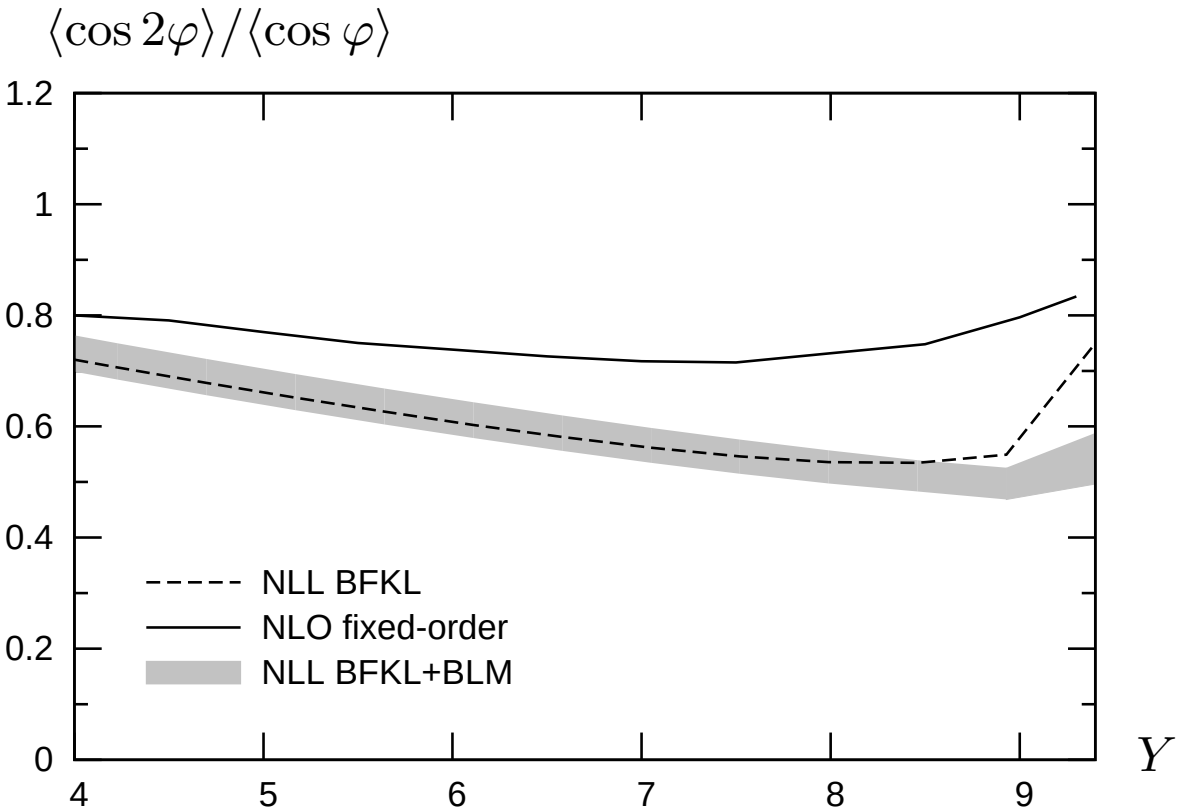

$35\,\mathrm{GeV} < |\mathbf{k}_{J1}| < 60\,\mathrm{GeV}$

$35\,\mathrm{GeV} < |\mathbf{k}_{J2}| < 60\,\mathrm{GeV}$

$50\,\mathrm{GeV} < \mathrm{Max}(|\mathbf{k}_{J1}|, |\mathbf{k}_{J2}|)$

$0 < |y_1| < 4.7$

$0 < |y_2| < 4.7$

Using BLM or not, there is a sizable difference between BFKL and fixed-order.

Comparison with fixed-order

Cross section: 13 TeV vs. 7 TeV

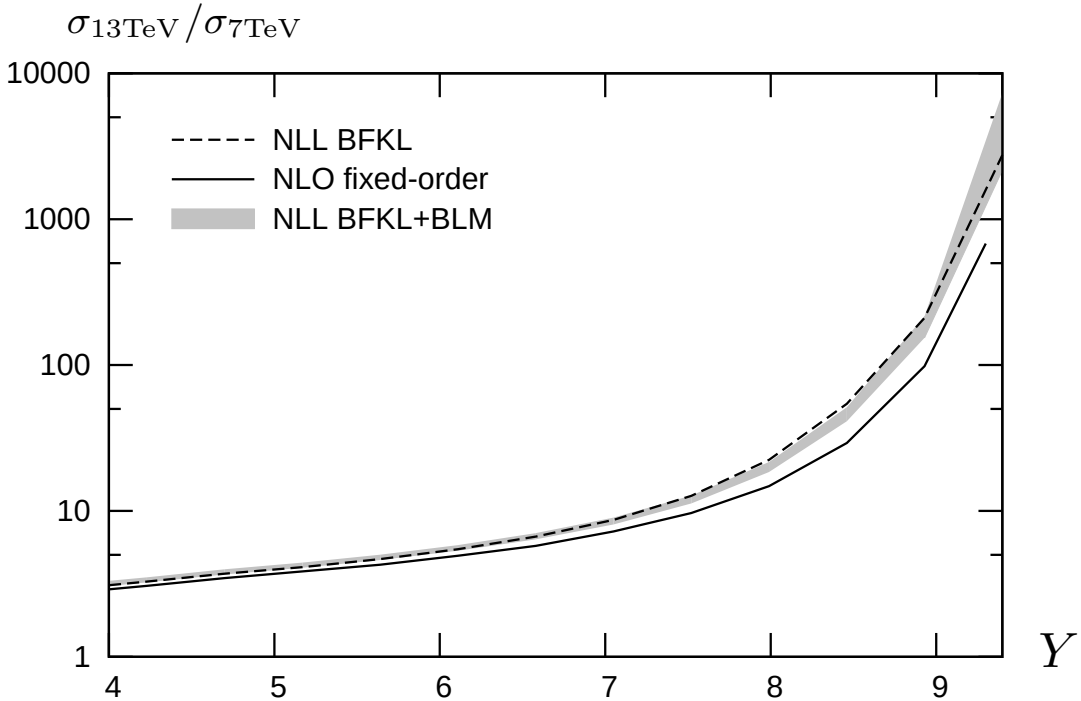

$$35\,\mathrm{GeV} < |\mathbf{k}_{J1}| < 60\,\mathrm{GeV}$$
$$35\,\mathrm{GeV} < |\mathbf{k}_{J2}| < 60\,\mathrm{GeV}$$
$$50\,\mathrm{GeV} < \mathrm{Max}(|\mathbf{k}_{J1}|, |\mathbf{k}_{J2}|)$$

$$0 < |y_1| < 4.7$$
$$0 < |y_2| < 4.7$$

- In a BFKL treatment, a strong rise of the cross section with increasing energy is expected.
- This rise is faster than in a fixed-order treatment

Energy-momentum conservation

- It is necessary to have $\mathbf{k}_{J\mathrm{min}1} \neq \mathbf{k}_{J\mathrm{min}2}$ for comparison with fixed order calculations but this can be problematic for BFKL because of energy-momentum conservation
- There is no strict energy-momentum conservation in BFKL
- This was studied at LO by Del Duca and Schmidt. They introduced an effective rapidity Y_{eff} defined as

$$Y_{\mathrm{eff}} \equiv Y \frac{\sigma^{2\to 3}}{\sigma^{\mathrm{BFKL},\mathcal{O}(\alpha_{\mathrm{s}}^3)}}$$

- When one replaces Y by Y_{eff} in the expression of σ^{BFKL} and truncates to $\mathcal{O}(\alpha_s^3)$, the exact $2 \to 3$ result is obtained

Energy-momentum conservation

We follow the idea of Del Duca and Schmidt, adding the NLO jet vertex contribution:

exact $2 \to 3$

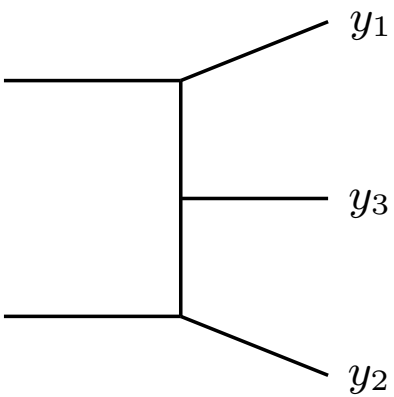

BFKL

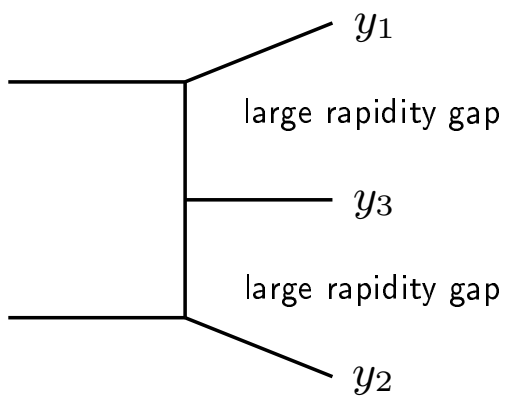

one emission from the Green's function + LO jet vertex

we have to take into account these additional $\mathcal{O}(\alpha_s^3)$ contributions:

+

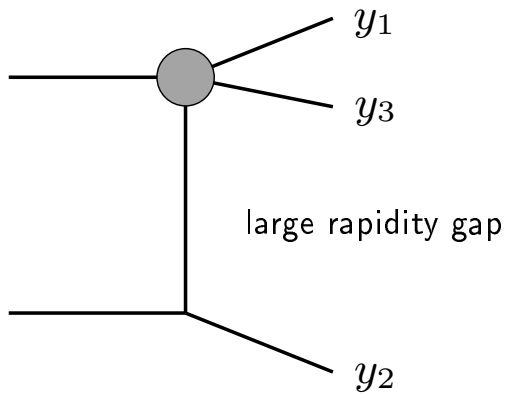

+

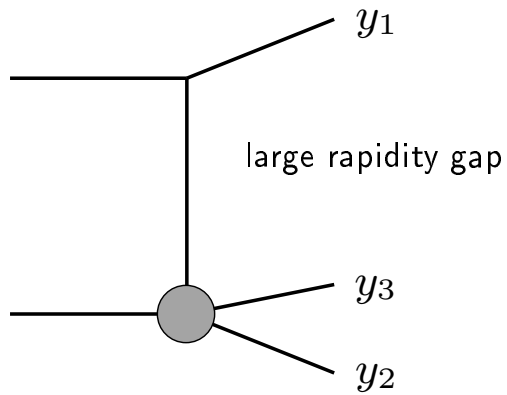

no emission from the Green's function + NLO jet vertex

Energy-momentum conservation

Variation of Y_{eff}/Y as a function of $\mathbf{k}_{J2}$ for fixed $\mathbf{k}_{J1} = 35$ GeV (with $\sqrt{s} = 7$ TeV, $Y = 8$):

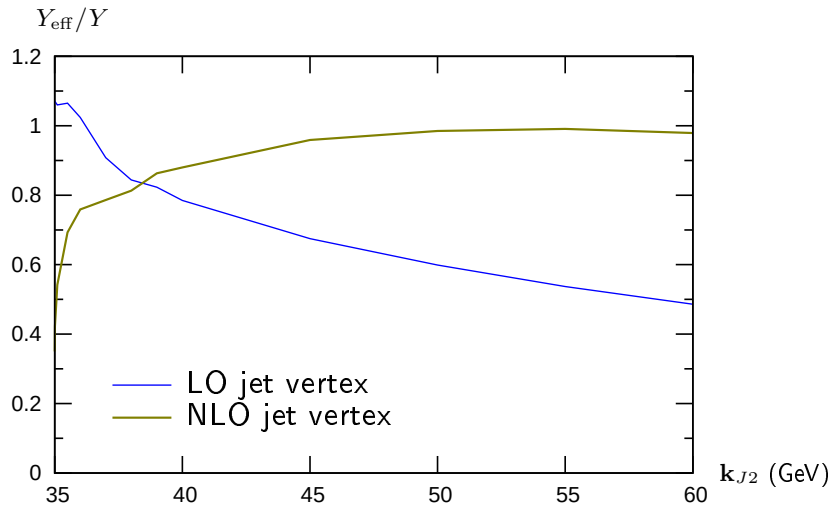

- With the LO jet vertex, Y_{eff} is much smaller than Y when $\mathbf{k}_{J1}$ and $\mathbf{k}_{J2}$ are significantly different
- This is the region important for comparison with fixed order calculations
- The improvement coming from the NLO jet vertex is very large in this region
- For $\mathbf{k}_{J1} = 35$ GeV and $\mathbf{k}_{J2} = 50$ GeV, typical of the values we used for comparison with fixed order, we get $\frac{Y_{\text{eff}}}{Y} \simeq 0.98$ at NLO vs. ~ 0.6 at LO

Can Mueller-Navelet jets be a manifestation of multiparton interactions?

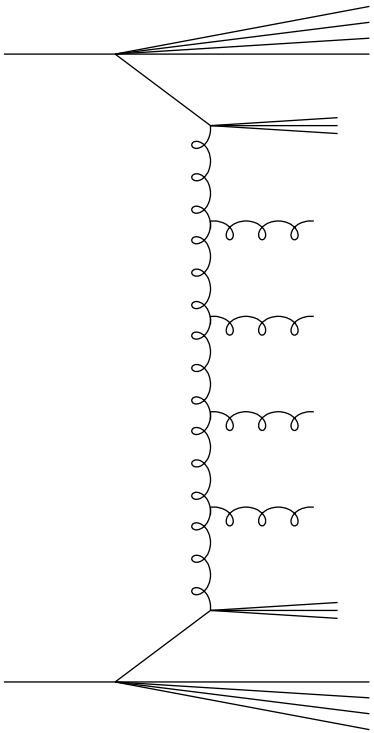

+

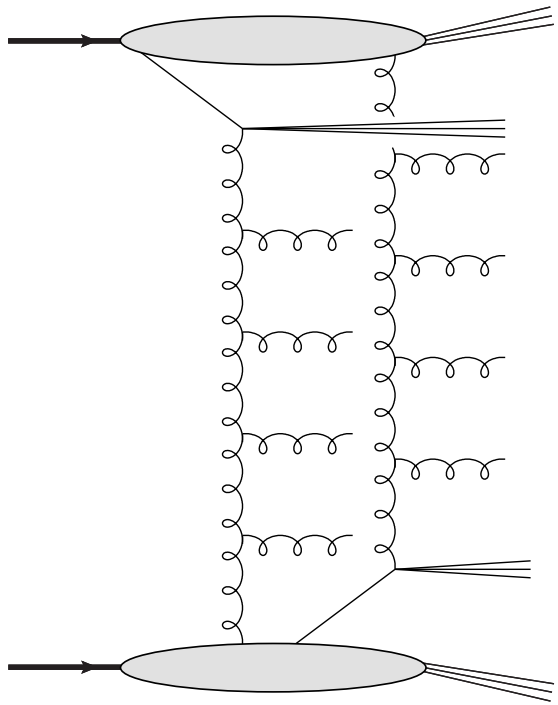

MN jets in the single partonic model

MN jets in MPI

here MPI = DPS (double parton scattering)

Can Mueller-Navelet jets be a manifestation of multiparton interactions?

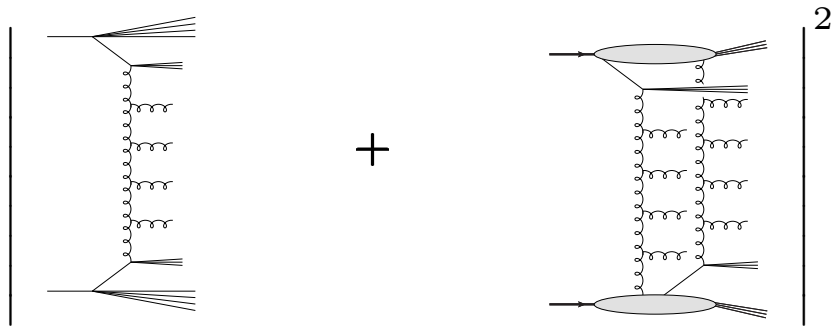

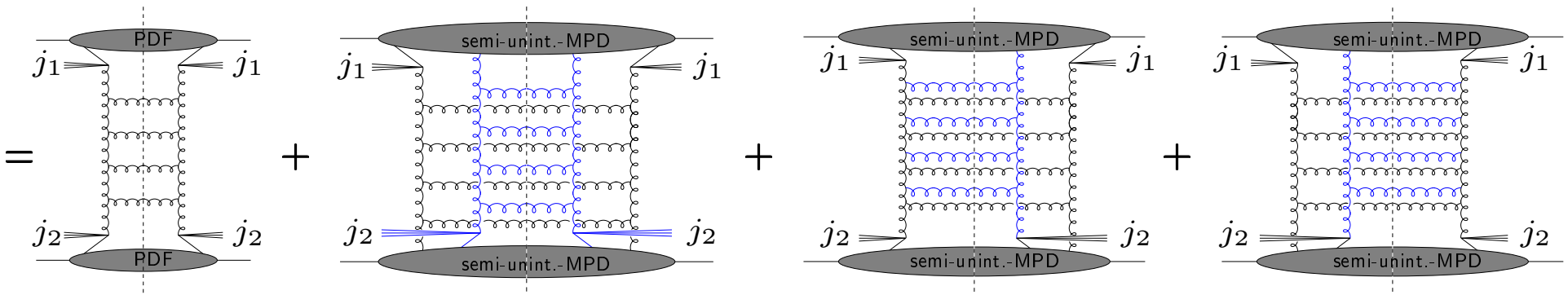

single $\mathbb{P}$ ladder | two $\mathbb{P}$ ladders | interferences

scaling: $s^{\alpha_{\mathbb{P}}}$ | $(??)\, s^{2\alpha_{\mathbb{P}}}$ | ??

- The twist counting is not easy for MPI kinds of contributions at small x
- $k_{\perp 1,2}$ are not integrated $\Rightarrow$ MPI may be competitive, and enhanced by small-x resummation
- Interference terms are not governed by BJKP (this is not a fully interacting 3-reggeons system) (for BJKP, $\alpha_{\mathbb{P}} < 1 \Rightarrow$ suppressed)

A phenomenological test: the problem

- Simplification: we neglect any interference contribution between the two mecchanisms
- How to evaluate the DPS contribution?

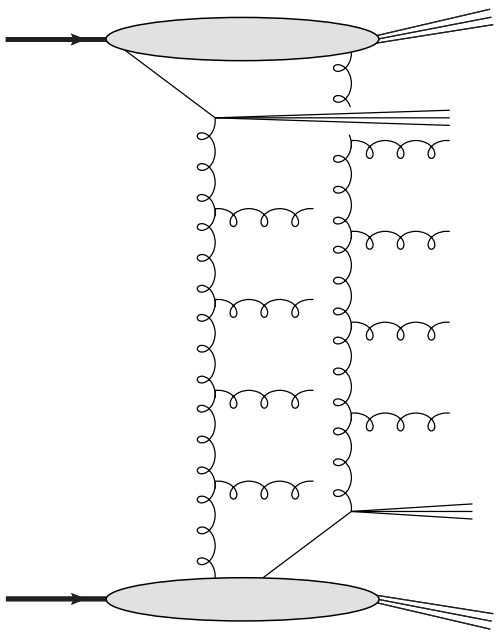

- This would require some kind of "hybrid" double parton distributions, with
  - one collinear parton
  - one off-shell parton (with some $k_\perp$)
- Almost nothing is known on such distributions

A phenomenological test: our ansatz

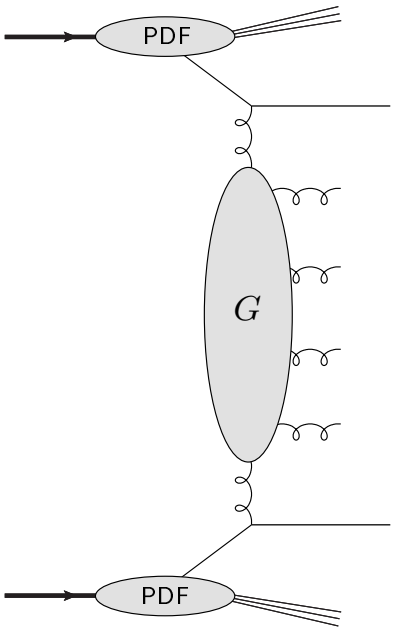

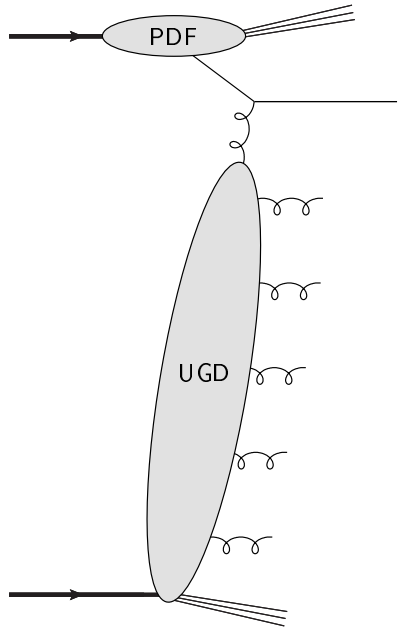

Mueller-Navelet jets production at LL accuracy

Inclusive forward jet production

Factorized ansatz for the DPS contribution:

$$\sigma_{\rm DPS} = \frac{\sigma_{\rm fwd}\ \sigma_{\rm bwd}}{\sigma_{\rm eff}}$$

Tevatron, LHC: $\sigma_{\rm eff} \simeq 15$ mb

To account for some discrepancy between various measurements, we take

$$\sigma_{\rm eff} \simeq 10 - 20 \text{ mb}$$

A phenomenological test: our ansatz

At LO for the jet vertex:

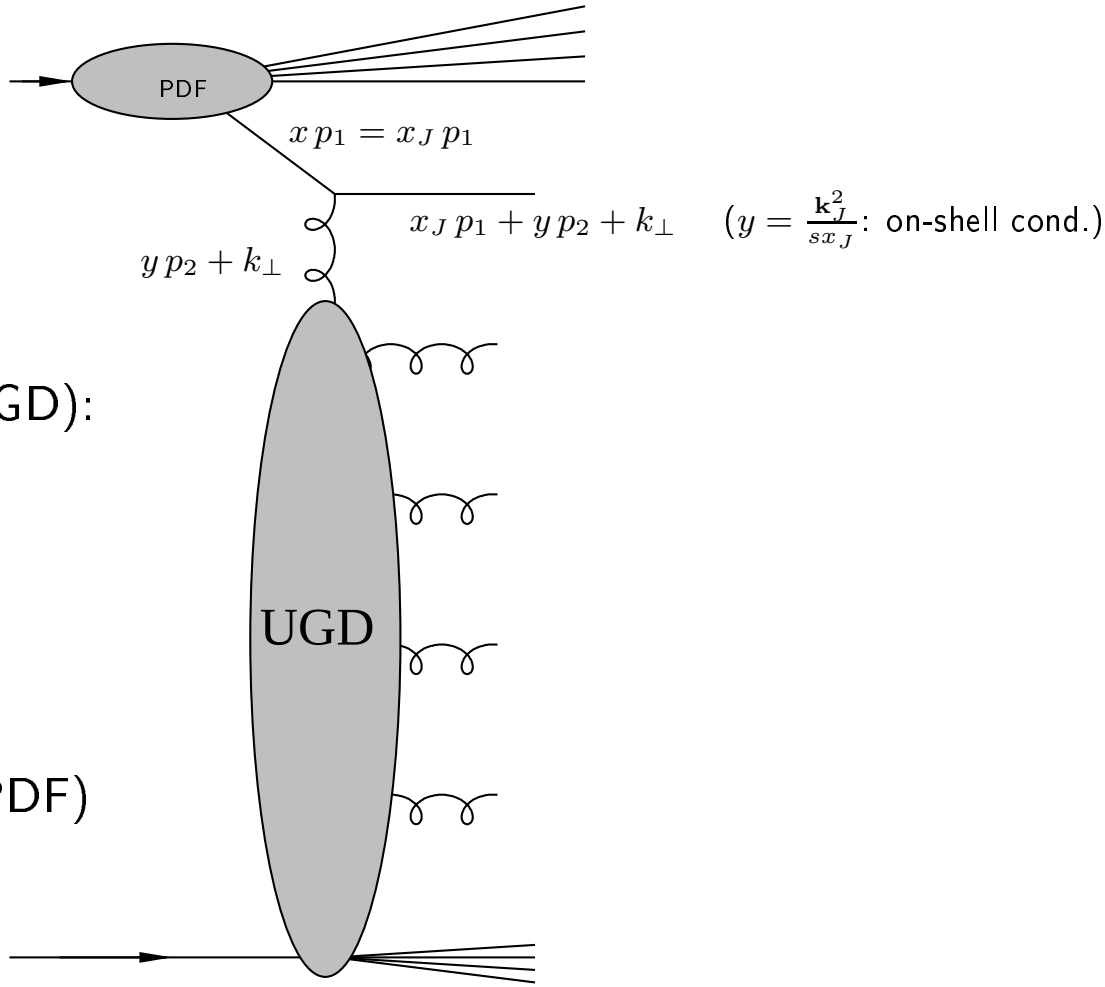

unintegrated gluon distribution (UGD):

$\mathcal{F}_g\left(\frac{\mathbf{k}_J^2}{s\,x_J}, |\mathbf{k}_J|\right)$

normalized according to:

$\int \mathrm{d}\mathbf{k}^2 \mathcal{F}_g(x, |\mathbf{k}|) = x f_g(x)$ (usual PDF)

inclusive forward jet cross-section:

$$\frac{\mathrm{d}\sigma}{\mathrm{d}|\mathbf{k}_J|\mathrm{d}y_J} = K\,\frac{\alpha_s}{|\mathbf{k}_J|}\,x_J\,(C_F\,f_q(x_J) + C_A\,f_g(x_J))\,\mathcal{F}_g\left(\frac{\mathbf{k}_J^2}{s\,x_J}, |\mathbf{k}_J|\right)$$

A phenomenological test

- We use CMS data at $\sqrt{s} = 7$ TeV, $3.2 < |y_J| < 4.7$
- We use various parametrization for the UGD
- For each parametrization we determine the range of K compatible with the CMS measurement in the lowest transverse momentum bin

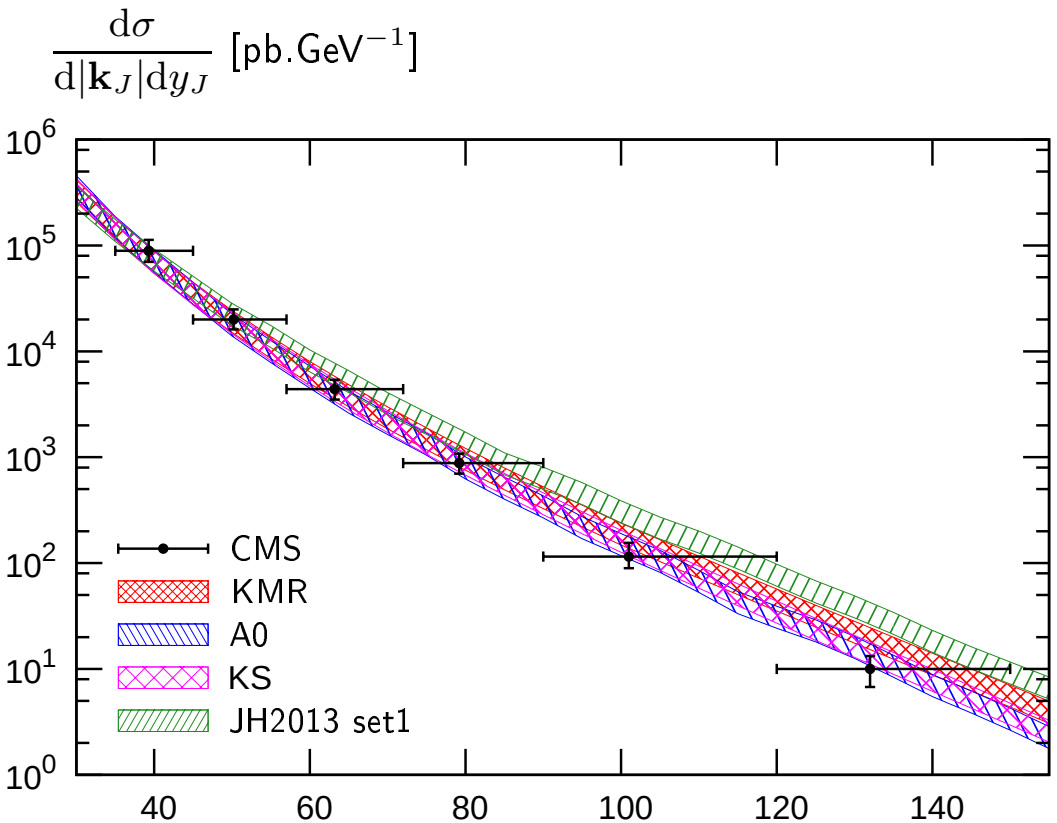

	K_{min}	K_{max}
KMS :	1.20	1.94
KMR :	1.05	1.69
A0 :	4.27	6.89
JH2013 :	2.44	3.94

$$\frac{d\sigma}{d|\mathbf{k}_J|dy_J} = K\,\frac{\alpha_s}{|\mathbf{k}_J|}\,x_J\,(C_F\,f_q(x_J) + C_A\,f_g(x_J))\,\mathcal{F}_g\left(\frac{\mathbf{k}_J^2}{s\,x_J}, |\mathbf{k}_J|\right)$$

SPS vs DPS: Results

We will focus on four choices of kinematical cuts:

- $\sqrt{s} = 7$ TeV, $|\mathbf{k}_{J1}| = |\mathbf{k}_{J2}| = 35$ GeV,
  (like in the CMS analysis for azimuthal correlations of MN jets)
- $\sqrt{s} = 14$ TeV, $|\mathbf{k}_{J1}| = |\mathbf{k}_{J2}| = 35$ GeV,
- $\sqrt{s} = 14$ TeV, $|\mathbf{k}_{J1}| = |\mathbf{k}_{J2}| = 20$ GeV,
- $\sqrt{s} = 14$ TeV, $|\mathbf{k}_{J1}| = |\mathbf{k}_{J2}| = 10$ GeV $\leftarrow$ highest DPS effect expected

parameters:

- $0 < y_{J,1} < 4.7$ and $-4.7 < y_{J,2} < 0$
- MSTW 2008 parametrization for PDFs
- In the case of the NLL NFKL calculation, anti-k_t jet algorithm with $R = 0.5$.

SPS vs DPS: cross-sections

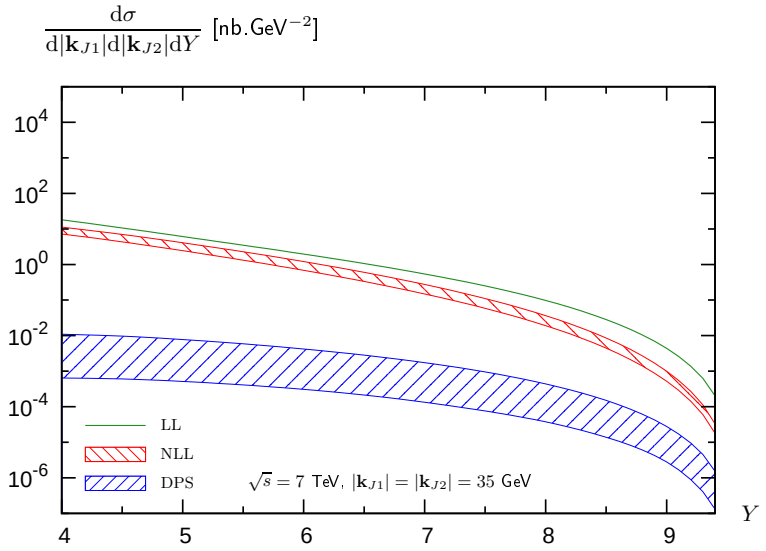

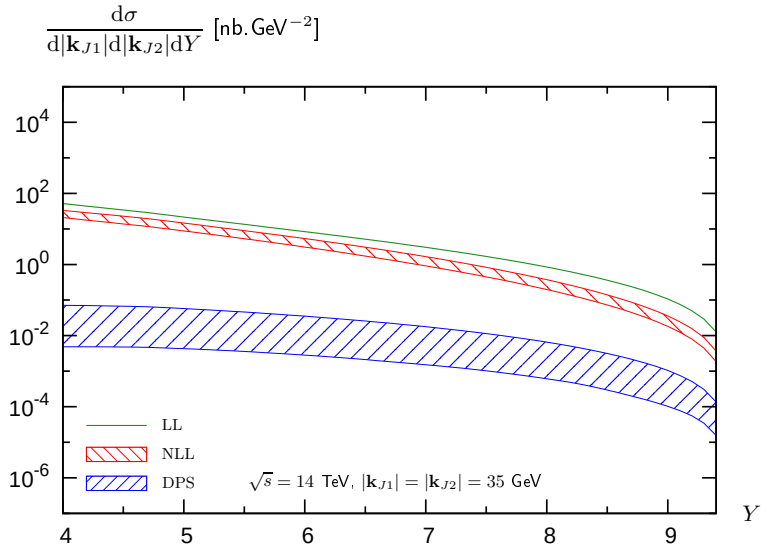

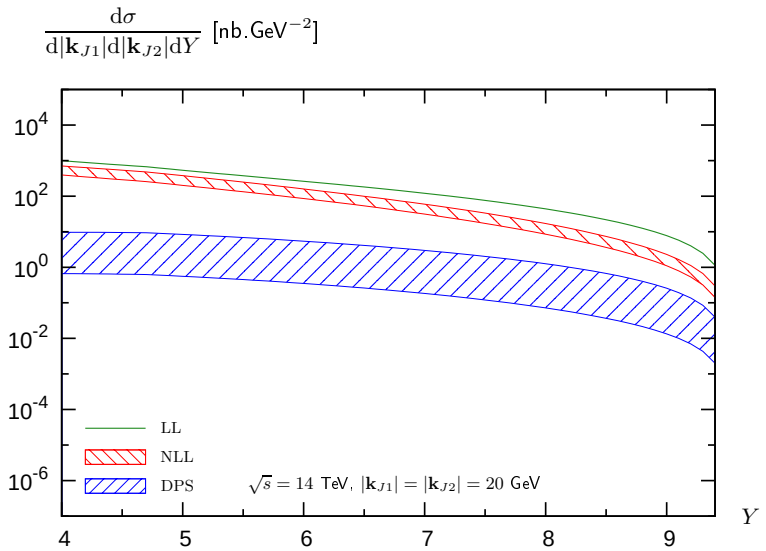

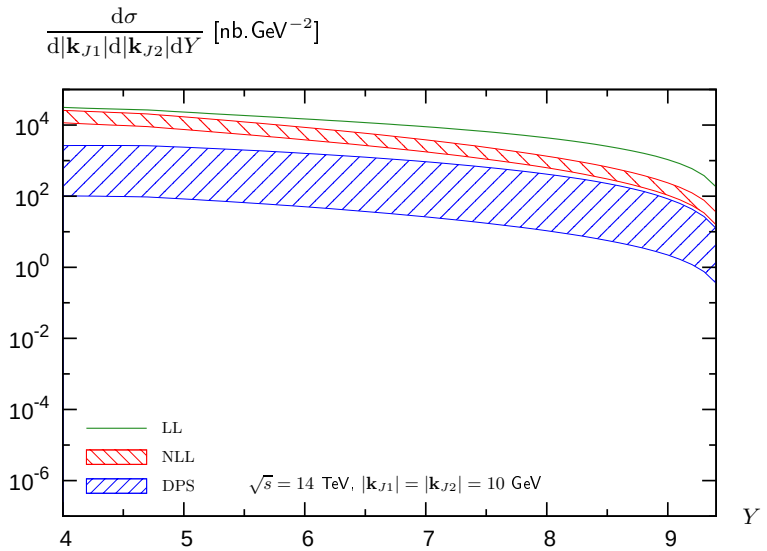

SPS vs DPS: cross-sections (ratios)

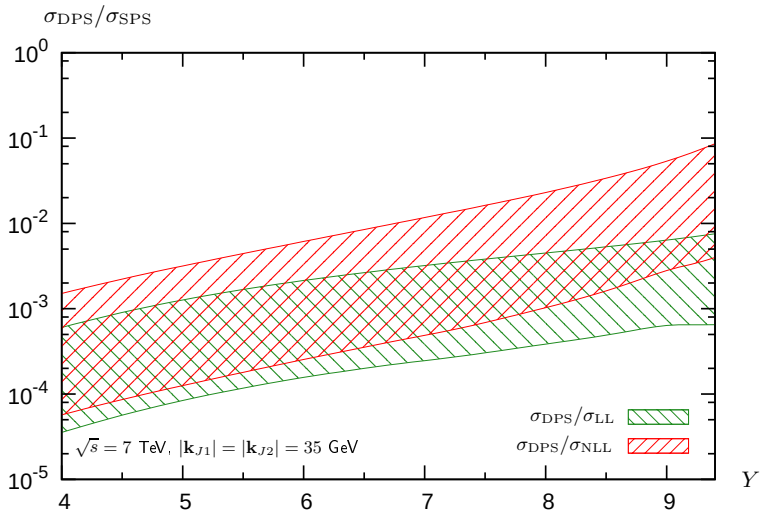

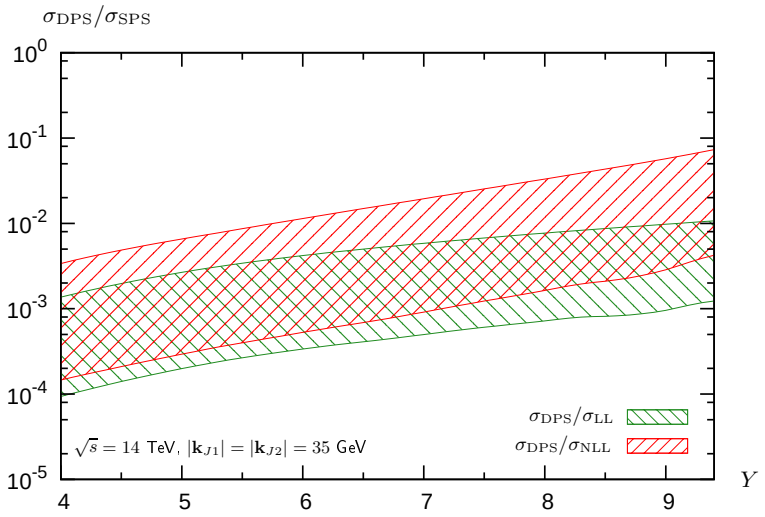

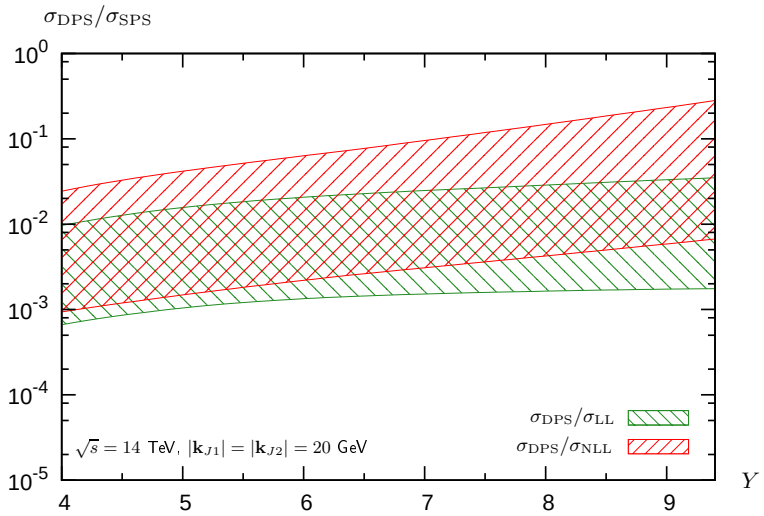

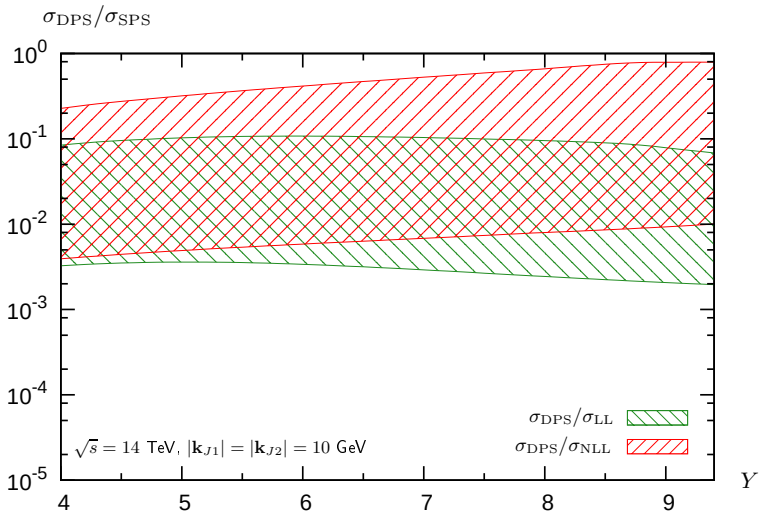

SPS vs DPS: Azimuthal correlations

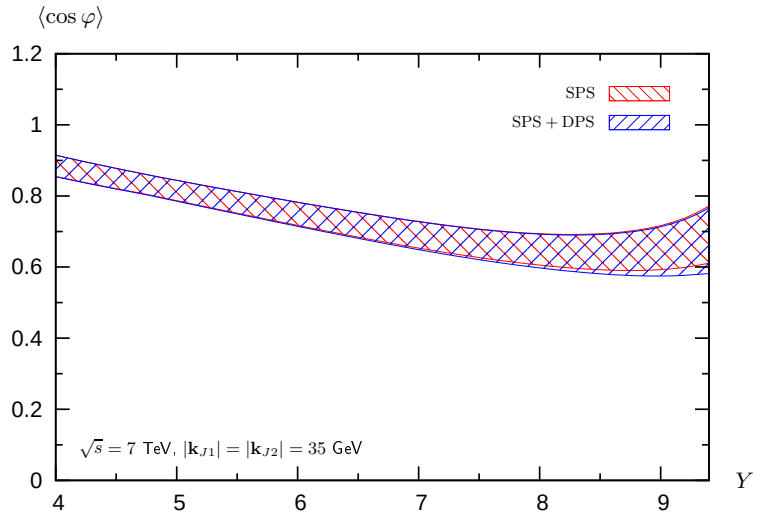

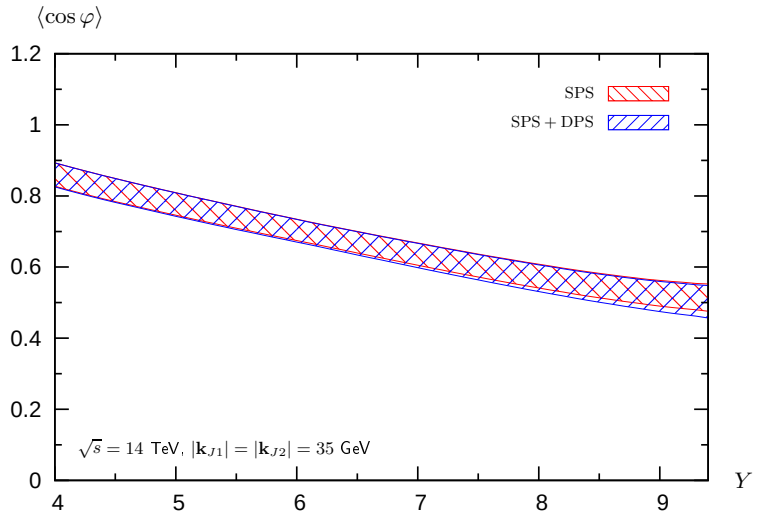

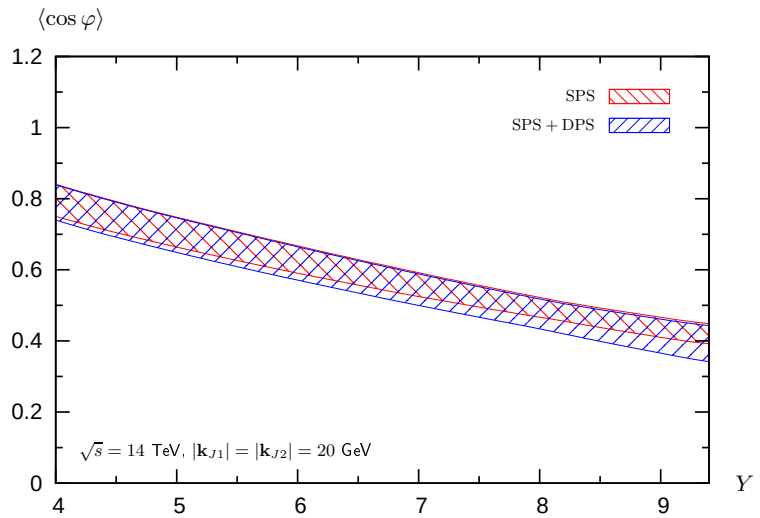

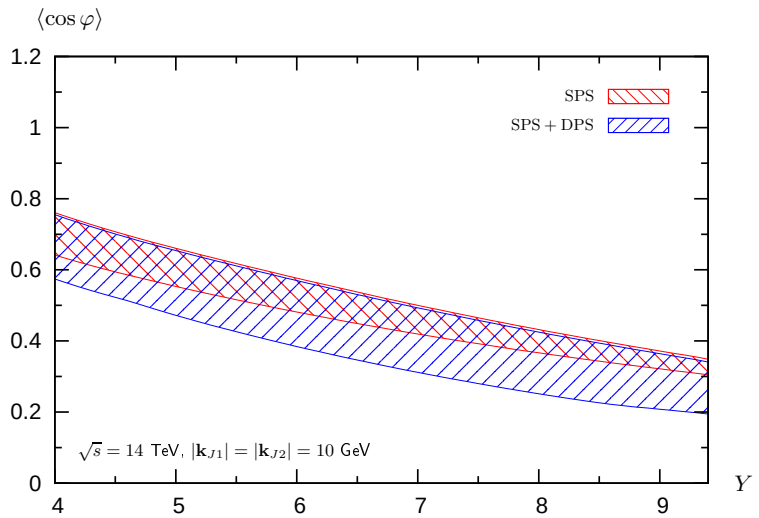

SPS vs DPS: Azimuthal distributions

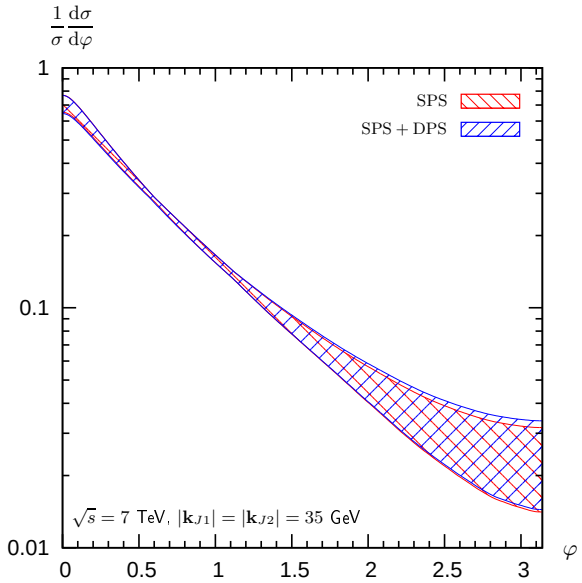

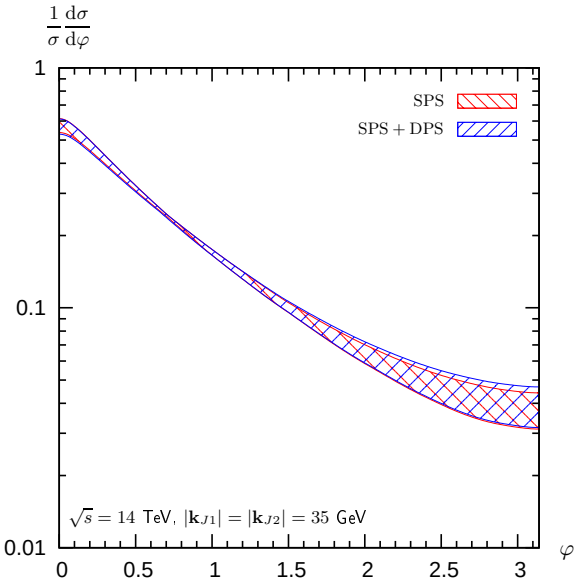

$8 < Y < 9.4$

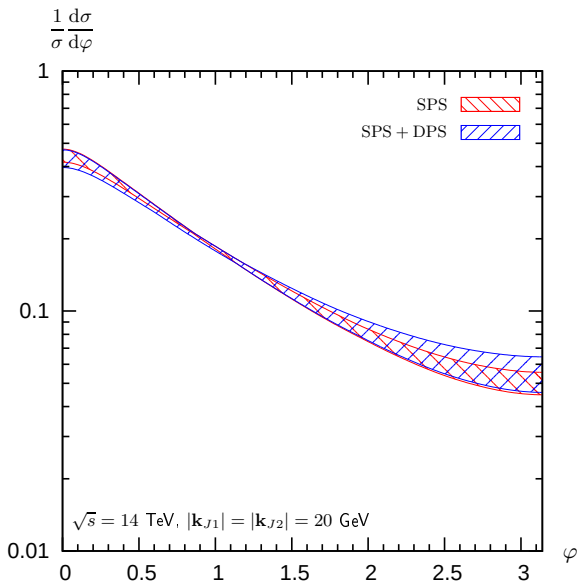

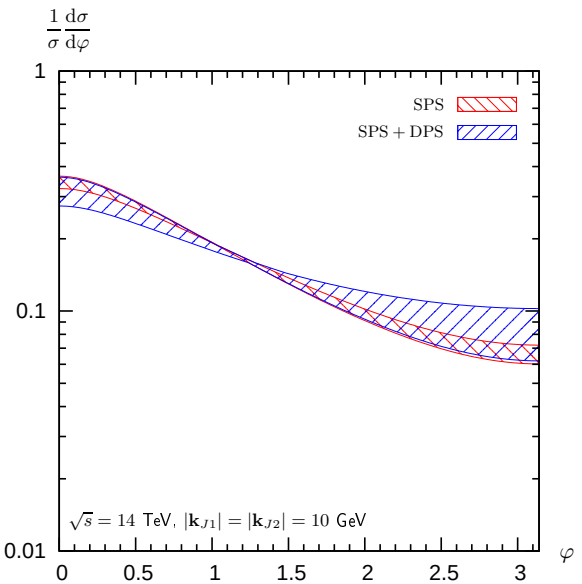

Inclusive production of a forward J/ψ + a backward jet

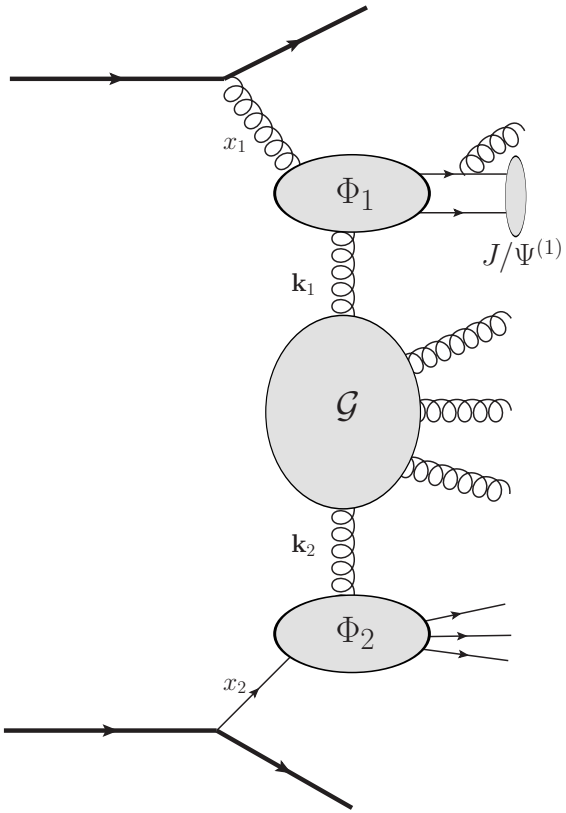

Color singlet mechanism

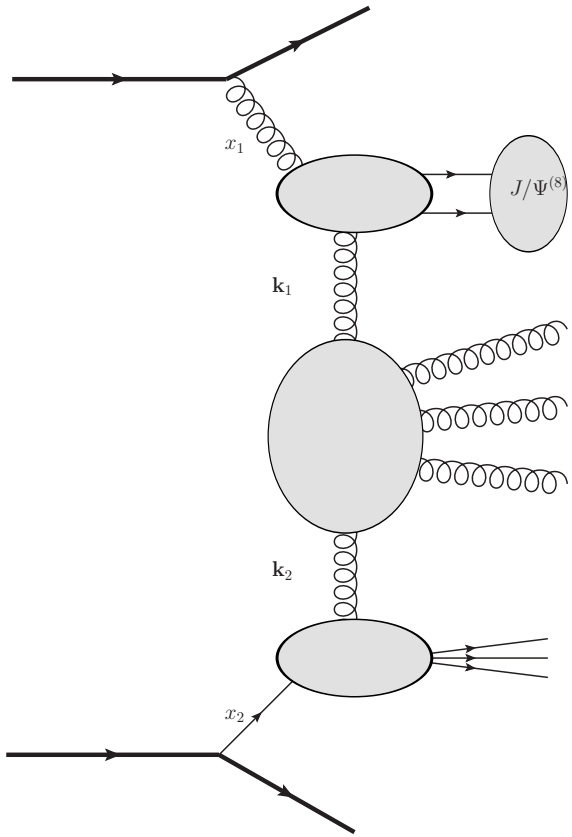

Color octet mechanism

- Hard scales: $\mathbf{k}_J$ and $M_{J/\psi}$
- Very promising at ATLAS (and CMS?)
- To be studied: cross-section study and azimuthal correlation

Work in progress with LO vertex + NLO BFKL Green function
R. Boussarie, B. Ducloué, L. Szymanowski, S. W.

Conclusions

- We studied Mueller-Navelet jets at full (vertex + Green's function) NLL BFKL accuracy and compared our results with the first data from the LHC
- The agreement with CMS data at 7 TeV is greatly improved by using the BLM scale fixing procedure
- $\langle \cos 2\varphi \rangle / \langle \cos \varphi \rangle$ is almost not affected by BLM and shows a clear difference between NLO fixed-order and NLL BFKL in an asymmetric configuration (this region is safer than the symmetric one...)
- Energy-momentum conservation seems to be less severely violated with the NLO jet vertex
- We did the same analysis at 13 TeV: [see backup slides]
  - Azimuthal decorrelations at 13 TeV vs 7 TeV are similar
  - NLL BFKL predicts a stronger rise of the cross section with increasing energy than a NLO fixed-order calculation

  Measurement of the cross section at $\sqrt{s} = 7$ or 8 TeV ?
- We studied the effect of DPS contributions which could mimic the MN jet
  - For cross-sections: The uncertainty on DPS is very large.
    Still, $\sigma_{DPS} < \sigma_{SPS}$ in the LHC kinematics
  - For angular correlations: including DPS does not significantly modify our NLL BFKL prediction
  - For low $\mathbf{k}_J$ and large Y, the effect of DPS can become larger than the uncertainty on the NLL BFKL calculation.
    One should focus on this region experimentally.

Third International Summer School of QCD

Dense systems in QCD at asymptotical energies

20th of June 2016 - 1st of July 2016

Laboratoire de Physique Théorique, Orsay

https://indico.in2p3.fr/event/12948/

- session: Formal developments in small-xBj physics: kT-factorization, saturation, color-glass condensate
  Dmitry Yu. Ivanov, Andrey V. Grabovsky, Heribert Weigert, Tolga Altinoluk, Stéphane Munier
- session: Formal developments in heavy ions physics
  François Gelis, Stéphane Peigné
- session: Phenomenological aspects
  Krzysztof Golec-Biernat, Javier L. Albacete, Elena Gonzalez Ferreiro
- session: Reconciling high-energy resummations with collinear factorization
  Bo-Wen Xiao

Organization committee:

Cyrille Marquet (CPhT, Palaiseau)

Kornelija Passek-Kumerički (Rudjer Bošković Institute, Zagreb)

Franck Sabatié (Irfu/SPhN, Gif-sur-Yvette) ***(chair)***

Lech Szymanowski (NCBJ, Warsaw)

Samuel Wallon (LPT, Orsay and UPMC, Paris) ***(chair)***

The school is financially supported by: **JSA Initiatives Fund Program, BNL, RBI-T-WINNING, GDR**

Backup

Comparison: 13 TeV vs. 7 TeV

Azimuthal correlation $\langle \cos \varphi \rangle$

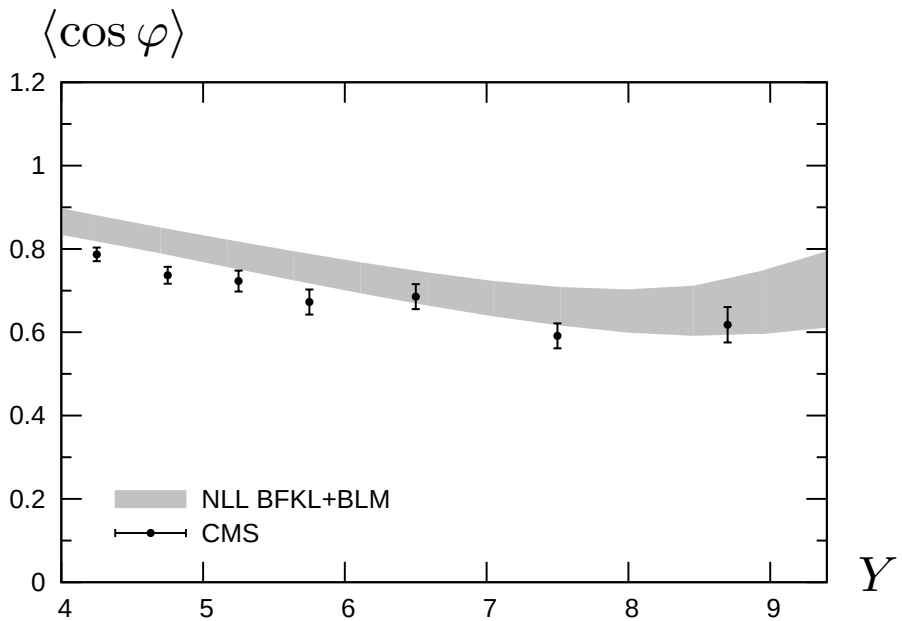

$\sqrt{s} = 7$ TeV

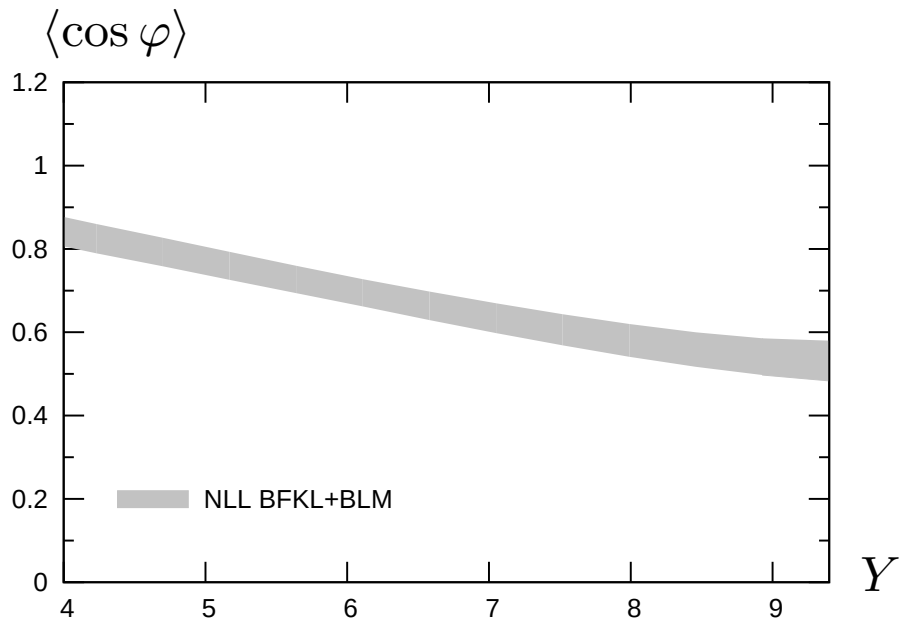

$\sqrt{s} = 13$ TeV

The behavior is similar at 13 TeV and at 7 TeV

Comparison: 13 TeV vs. 7 TeV

Azimuthal distribution (integrated over $6 < Y < 9.4$)

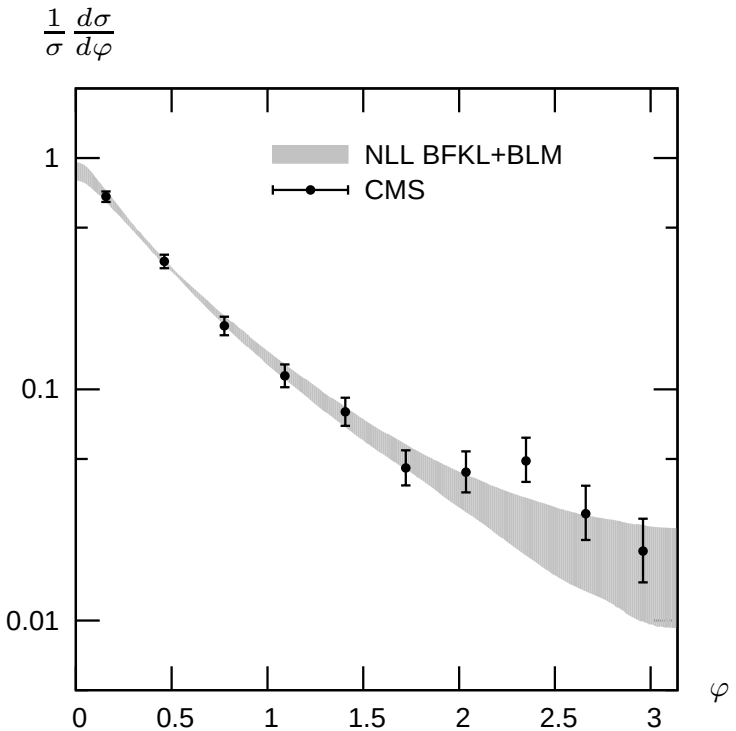

$\sqrt{s} = 7$ TeV

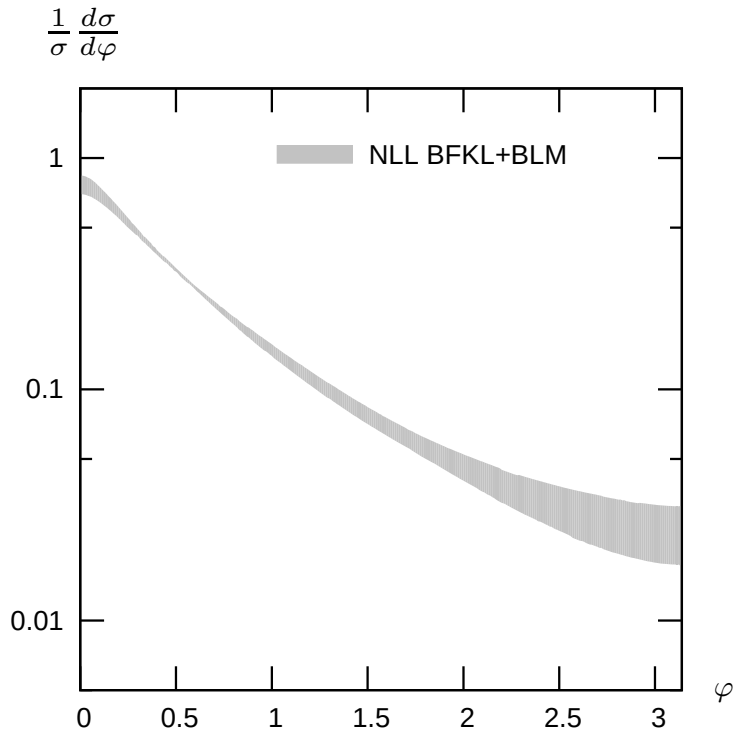

$\sqrt{s} = 13$ TeV

The behavior is similar at 13 TeV and at 7 TeV

Comparison: 13 TeV vs. 7 TeV

Azimuthal correlation $\langle \cos 2\varphi \rangle / \langle \cos \varphi \rangle$

(asymmetric configuration)

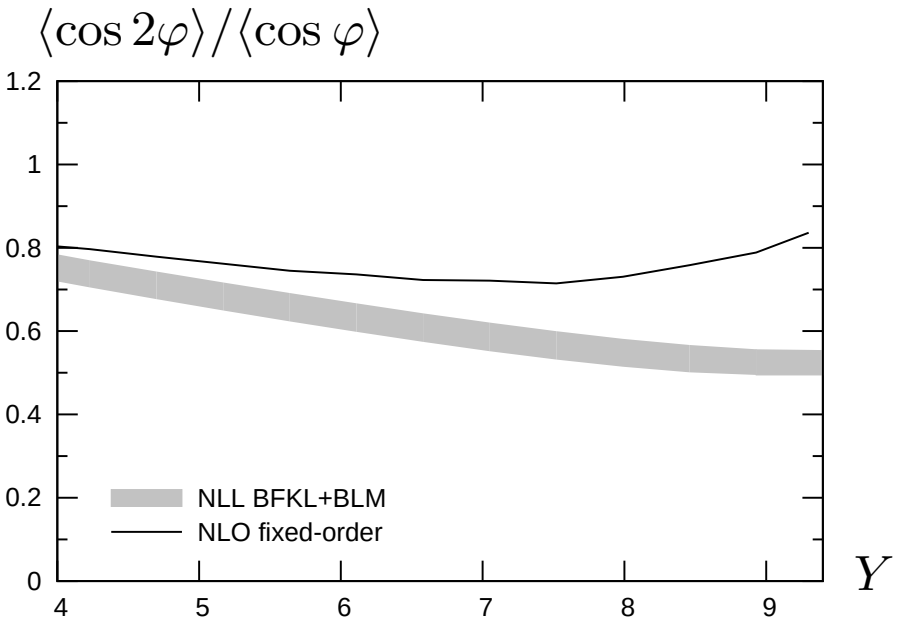

$\sqrt{s} = 7$ TeV

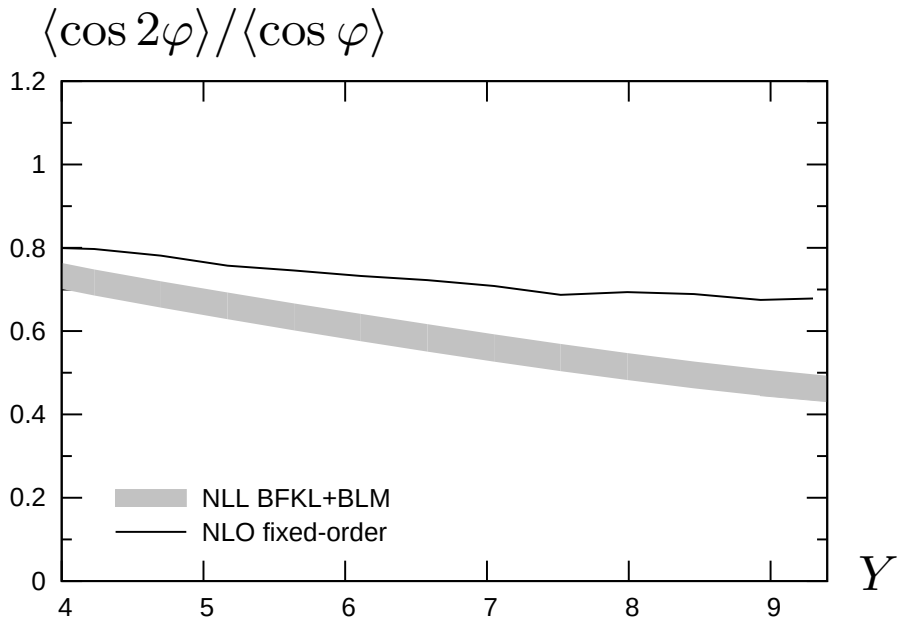

$\sqrt{s} = 13$ TeV

The difference between BFKL and fixed-order is smaller at 13 TeV than at 7 TeV

Comparison: 13 TeV vs. 7 TeV

Cross section

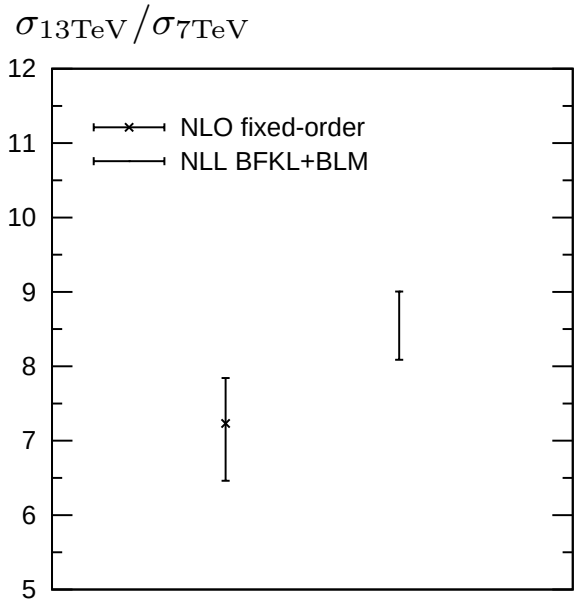

$Y = 7$

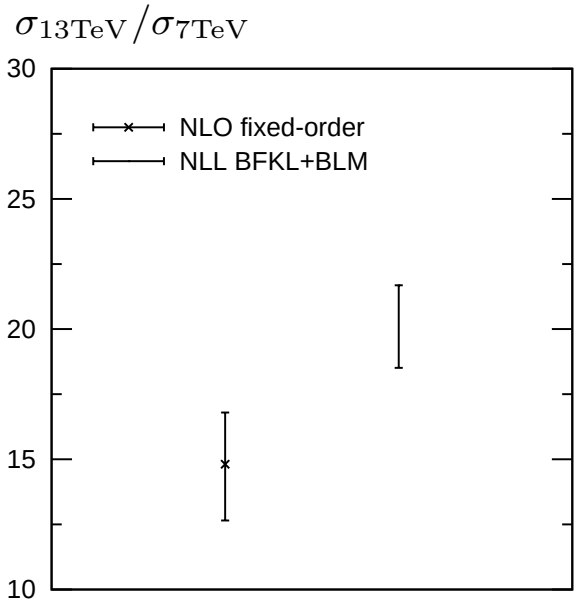

$Y = 8$

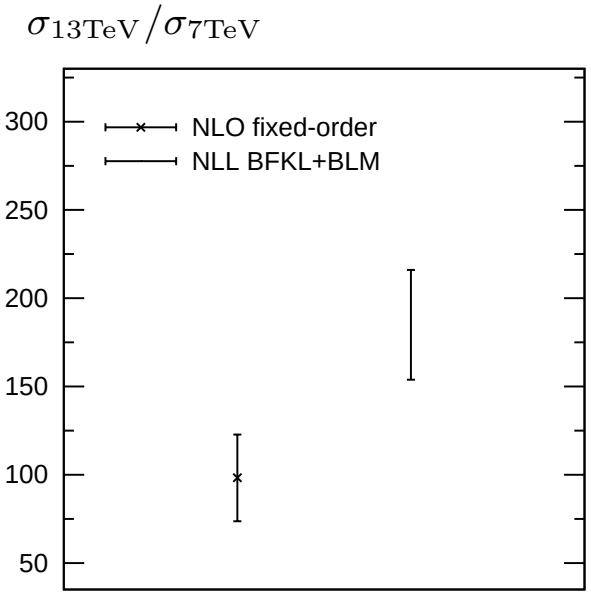

$Y = 9$

Master formulas

It is useful to define the coefficients $\mathcal{C}_n$ as

$$\begin{aligned}\mathcal{C}_n \quad \equiv \quad & \int \mathrm{d}\phi_{J1}\,\mathrm{d}\phi_{J2}\,\cos\left(n(\phi_{J1}-\phi_{J2}-\pi)\right) \\ & \times \int \mathrm{d}^2\mathbf{k}_1\,\mathrm{d}^2\mathbf{k}_2\,\Phi(\mathbf{k}_{J1},x_{J1},-\mathbf{k}_1)\,G(\mathbf{k}_1,\mathbf{k}_2,\hat{s})\,\Phi(\mathbf{k}_{J2},x_{J2},\mathbf{k}_2)\end{aligned}$$

- $n=0 \Longrightarrow$ differential cross-section

$$\mathcal{C}_0 = \frac{\mathrm{d}\sigma}{\mathrm{d}|\mathbf{k}_{J1}|\,\mathrm{d}|\mathbf{k}_{J2}|\,\mathrm{d}y_{J1}\,\mathrm{d}y_{J2}}$$

- $n>0 \Longrightarrow$ azimuthal decorrelation

$$\frac{\mathcal{C}_n}{\mathcal{C}_0} = \langle\cos\left(n(\phi_{J,1}-\phi_{J,2}-\pi)\right)\rangle \equiv \langle\cos(n\varphi)\rangle$$

- sum over $n \Longrightarrow$ azimuthal distribution

$$\frac{1}{\sigma}\frac{d\sigma}{d\varphi} \;=\; \frac{1}{2\pi}\left\{1+2\sum_{n=1}^{\infty}\cos\left(n\varphi\right)\langle\cos\left(n\varphi\right)\rangle\right\}$$

Master formulas in conformal variables

Rely on LL BFKL eigenfunctions

- LL BFKL eigenfunctions: $E_{n,\nu}(\mathbf{k}_1) = \frac{1}{\pi\sqrt{2}} \left(\mathbf{k}_1^2\right)^{i\nu-\frac{1}{2}} e^{in\phi_1}$
- decompose Φ on this basis
- use the known LL eigenvalue of the BFKL equation on this basis:

$$\omega(n,\nu) = \bar{\alpha}_s \chi_0\left(|n|, \tfrac{1}{2} + i\nu\right)$$

with $\chi_0(n,\gamma) = 2\Psi(1) - \Psi\left(\gamma + \frac{n}{2}\right) - \Psi\left(1 - \gamma + \frac{n}{2}\right)$

$(\Psi(x) = \Gamma'(x)/\Gamma(x),\ \bar{\alpha}_s = N_c \alpha_s/\pi)$

- $\Longrightarrow$ master formula:

$$\mathcal{C}_m = (4 - 3\,\delta_{m,0}) \int \mathrm{d}\nu\, C_{m,\nu}(|\mathbf{k}_{J1}|, x_{J,1})\, C^*_{m,\nu}(|\mathbf{k}_{J2}|, x_{J,2}) \left(\frac{\hat{s}}{s_0}\right)^{\omega(m,\nu)}$$

$$\text{with} \quad C_{m,\nu}(|\mathbf{k}_J|, x_J) = \int \mathrm{d}\phi_J\, \mathrm{d}^2\mathbf{k}\, \mathrm{d}x\, f(x) V(\mathbf{k}, x) E_{m,\nu}(\mathbf{k}) \cos(m\phi_J)$$

- at NLL, same master formula: just change $\omega(m,\nu)$ and V
  (although $E_{n,\nu}$ are not anymore eigenfunctions)
- one may improve the NLL BFKL kernel by imposing its compatibility with DGLAP in the (anti)collinear limit (poles in $\gamma = 1/2 + i\nu$ plane)
  Salam; Ciafaloni, Colferai
  note: NLL vertices are free of γ poles

Numerical implementation

In practice: two codes have been developed

A *Mathematica* code, exploratory

D. Colferai, F. Schwennsen, L. Szymanowski, S. W.
JHEP 1012:026 (2010) 1-72 [arXiv:1002.1365 [hep-ph]]

- jet cone-algorithm with $R = 0.5$
- MSTW 2008 PDFs (available as *Mathematica* packages)
- $\mu_R = \mu_F$ (in MSTW 2008 PDFs); we take $\mu_R = \mu_F = \sqrt{|\mathbf{k}_{J1}|\,|\mathbf{k}_{J2}|}$
- two-loop running coupling $\alpha_s(\mu_R^2)$
- we use a ν grid (with a dense sampling around 0)
- we use Cuba integration routines (in practice Vegas): precision 10^{-2} for 500.000 max points per integration
- mapping $|\mathbf{k}| = |\mathbf{k}_J| \tan(\xi\pi/2)$ for $\mathbf{k}$ integrations $\Rightarrow [0, \infty[\to [0, 1]$
- although formally the results should be finite, it requires a special grouping of the integrand in order to get stable results
  $\Longrightarrow$ 14 minimal stable basic blocks to be evaluated numerically
- rather slow code

Numerical implementation

A *Fortran* code, $\simeq 20$ times faster

B. Ducloué, L. Szymanowski, S.W.

JHEP 05 (2013) 096 [arXiv:1207.7012 [hep-ph]]

- Check of our *Mathematica* based results
- Detailled check of previous mixed studies (NLL Green's function + LL jet vertices)
- Allows for k_J integration in a finite range
- Stability studies (PDFs, etc...) made easier
- Comparison with the recent small R study of D. Yu. Ivanov, A. Papa
- Azimuthal distribution
- More detailled comparison with fixed order NLO:
  there is a hope to distinguish NLL BFKL / NLO fixed order
- Problems remain with ν integration for low Y
  (for $Y < \frac{\pi}{2\alpha_s N_c} \sim 4$). To be fixed!

  We restrict ourselves to $Y > 4$.

Integration over $|\mathbf{k}_J|$

Experimental data is integrated over some range, $k_{J\mathbf{min}} \leq k_J = |\mathbf{k}_J|$

Growth of the cross section with increasing $k_{J\mathbf{max}}$:

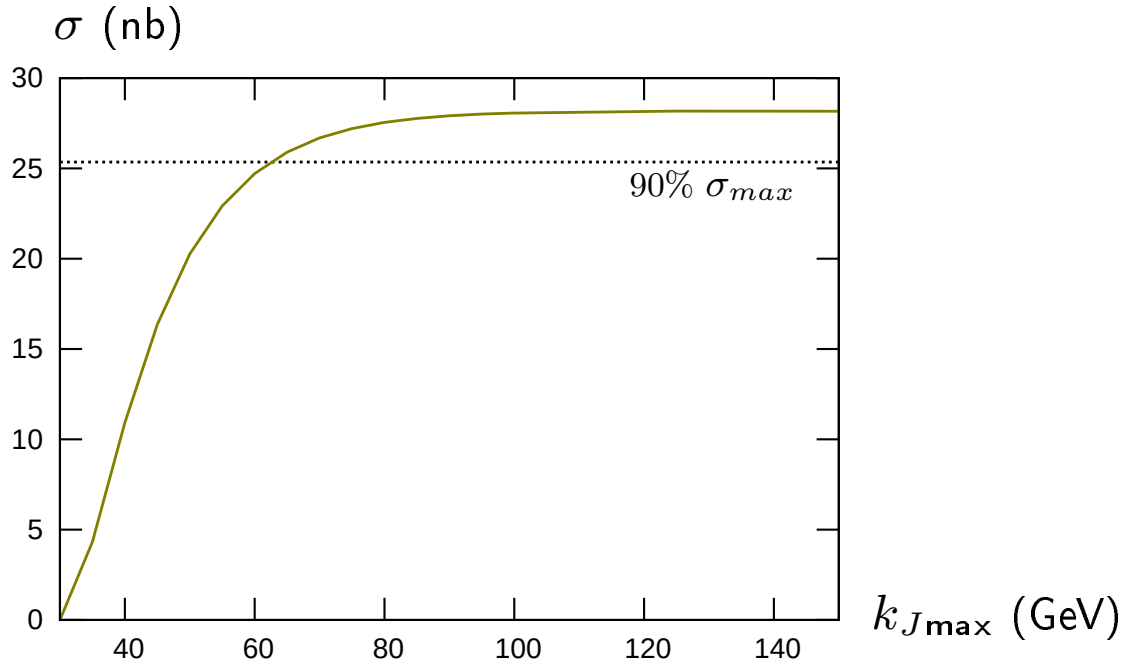

$\Rightarrow$ need to integrate up to $k_{J\mathbf{max}} \sim 60$ GeV

A consistency check of stability of $|\mathbf{k}_J|$ integration have been made:

- consider the simplified NLL Green's function + LL jet vertices scenario
- the integration $\int_{k_{J\,min}}^{\infty} dk_J$ can be performed analytically
- comparison with integrated results of Sabio Vera, Schwennsen is safe

Results: symmetric configuration ($|\mathbf{k}_{J,1\,\mathrm{min}}| = |\mathbf{k}_{J,2\,\mathrm{min}}| = 35\,\mathrm{GeV}$) $\sqrt{s} = 7$ TeV

Azimuthal distribution

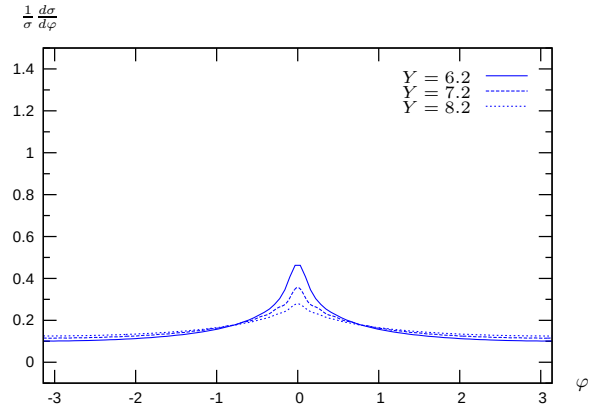

pure LL

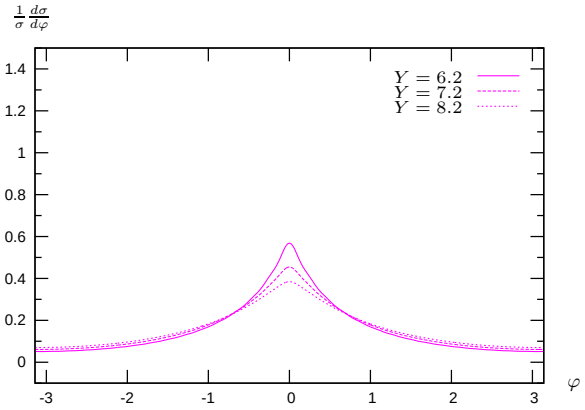

LL vertices + NLL Green's fun.

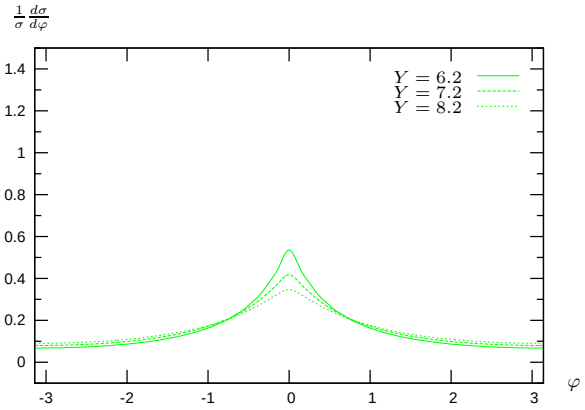

LL vert. + NLL resum. Green's fun.

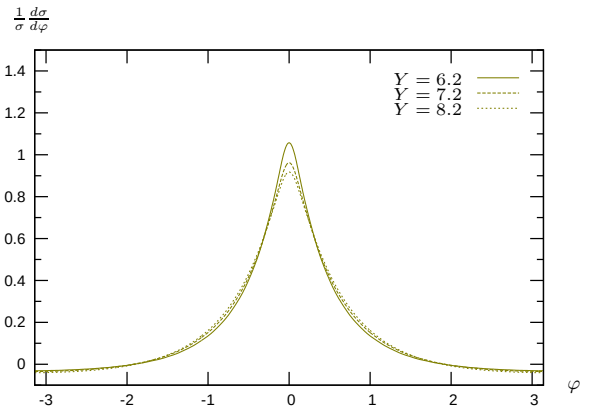

NLL vert. + NLL Green's fun.

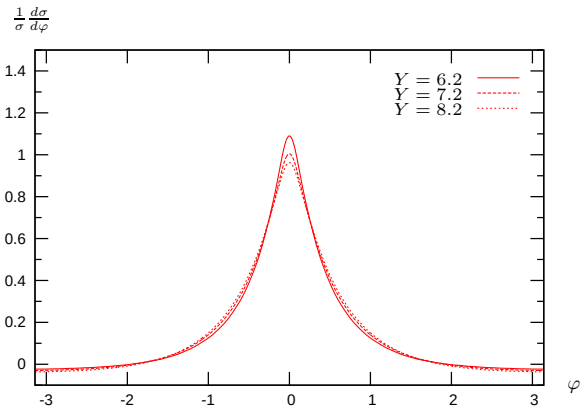

NLL vert. + NLL resum. Green's fun.

$$35\,\mathrm{GeV} < |\mathbf{k}_{J1}| < 60\,\mathrm{GeV}$$
$$35\,\mathrm{GeV} < |\mathbf{k}_{J2}| < 60\,\mathrm{GeV}$$

$$0 < Y_1 < 4.7$$
$$0 < Y_2 < 4.7$$

Full NLL treatment predicts :

- Less decorrelation for the same Y
- Slower decorrelation with increasing Y

Results: symmetric configuration ($|\mathbf{k}_{J,1\,\mathrm{min}}| = |\mathbf{k}_{J,2\,\mathrm{min}}| = 35\,\mathrm{GeV}$) $\sqrt{s} = 7$ TeV

Azimuthal distribution: stability with respect to s_0 and $\mu_R = \mu_F$

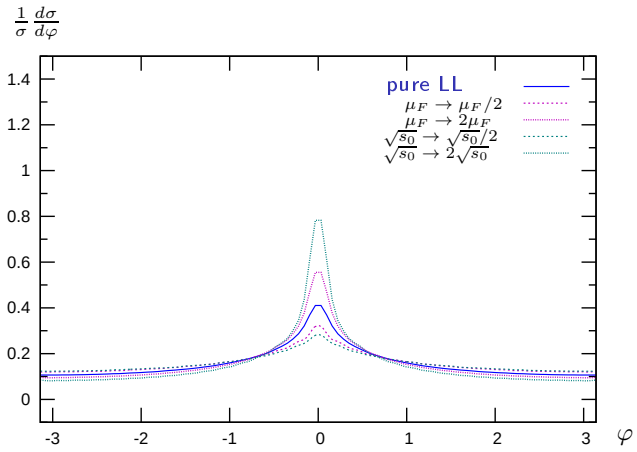

pure LL

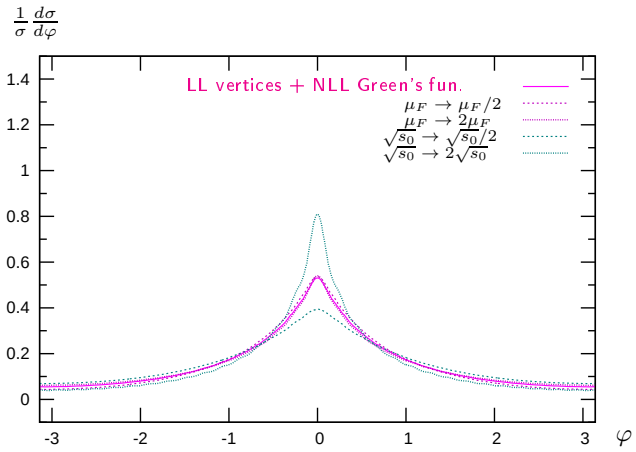

LL vertices + NLL Green's fun.

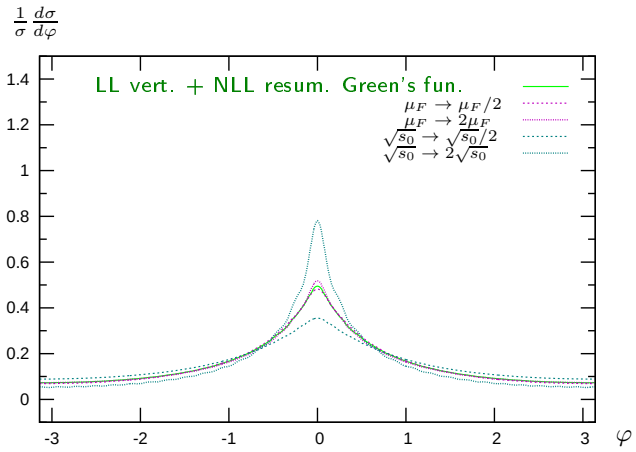

LL vert. + NLL resum. Green's fun.

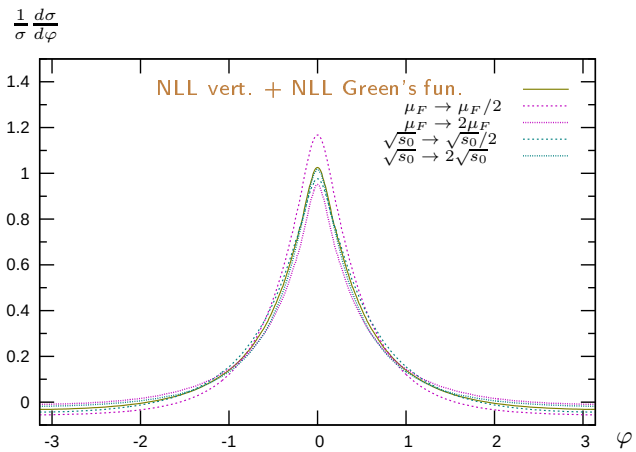

NLL vert. + NLL Green's fun.

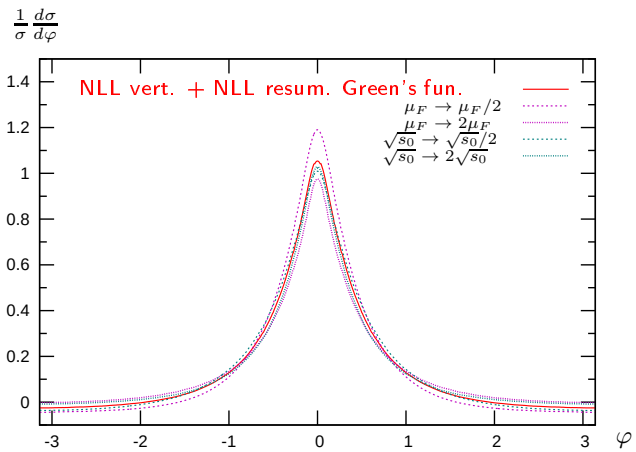

NLL vert. + NLL resum. Green's fun.

$35\,\mathrm{GeV} < |\mathbf{k}_{J1}| < 60\,\mathrm{GeV}$
$35\,\mathrm{GeV} < |\mathbf{k}_{J2}| < 60\,\mathrm{GeV}$

$0 < Y_1 < 4.7$
$0 < Y_2 < 4.7$
integrating on the bin:
$6 < Y = Y_1 + Y_2 < 9.4$

The predicted φ distribution within full NLL treatment is stable

Jet vertex: LL versus NLL

$\mathbf{k}, \mathbf{k}'$ = Euclidian two dimensional vectors

LL jet vertex:

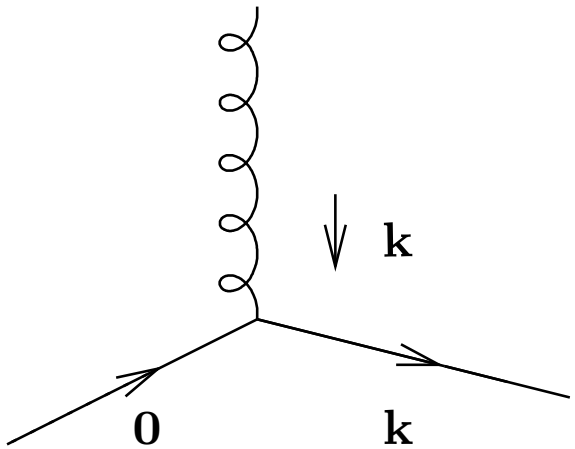

NLL jet vertex:

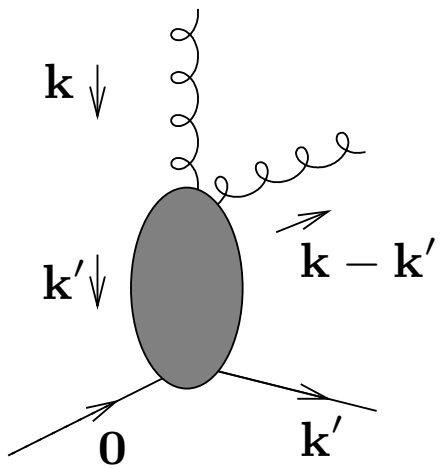

Jet algorithms

- a jet algorithm should be IR safe, both for soft and collinear singularities
- the most common jet algorithm are:
  - k_t algorithms (IR safe but time consuming for multiple jets configurations)
  - cone algorithm (not IR safe in general; can be made IR safe at NLO: Ellis, Kunszt, Soper)

Jet vertex: jet algorithms

Cone jet algorithm at NLO (Ellis, Kunszt, Soper)

- Should partons $(|\mathbf{p}_1|, \phi_1, y_1)$ and $(\mathbf{p}_2|, \phi_2, y_2)$ combined in a single jet? $|\mathbf{p}_i|$ =transverse energy deposit in the calorimeter cell i of parameter $\Omega = (y_i, \phi_i)$ in $y - \phi$ plane
- define transverse energy of the jet: $p_J = |\mathbf{p}_1| + |\mathbf{p}_2|$
- jet axis:

$$\Omega_c \begin{cases} y_J = \dfrac{|\mathbf{p}_1|\, y_1 + |\mathbf{p}_2|\, y_2}{p_J} \\ \phi_J = \dfrac{|\mathbf{p}_1|\, \phi_1 + |\mathbf{p}_2|\, \phi_2}{p_J} \end{cases}$$

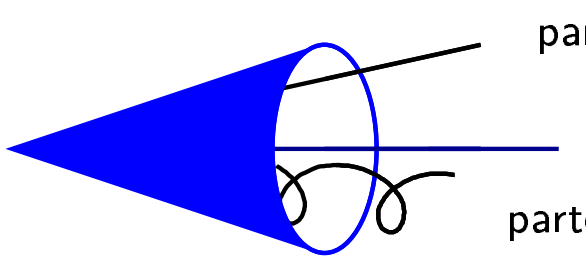

$\Omega = (y_i, \phi_i)$ in $y - \phi$ plane

If distances $|\Omega_i - \Omega_c|^2 \equiv (y_i - y_c)^2 + (\phi_i - \phi_c)^2 < R^2$ $(i = 1$ and $i = 2)$

$\Longrightarrow$ partons 1 and 2 are in the same cone Ω_c

combined condition: $|\Omega_1 - \Omega_2| < \dfrac{|\mathbf{p}_1| + |\mathbf{p}_2|}{max(|\mathbf{p}_1|, |\mathbf{p}_2|)} R$

LL jet vertex and cone algorithm

$\mathbf{k}, \mathbf{k}'$ = Euclidian two dimensional vectors

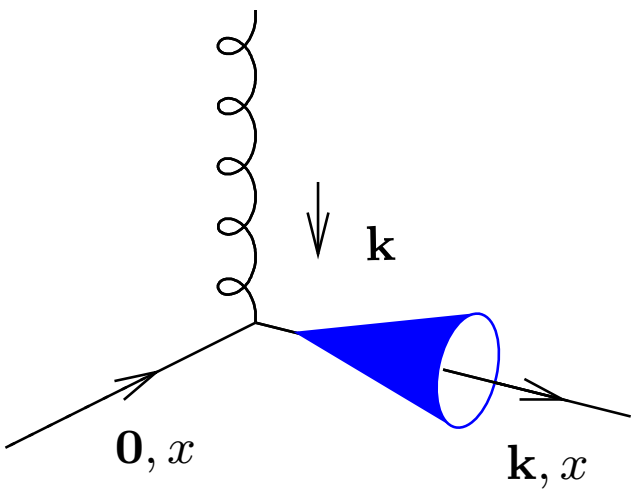

$$\mathcal{S}_J^{(2)}(k_\perp; x) = \delta\left(1 - \frac{x_J}{x}\right) |\mathbf{k}| \, \delta^{(2)}(\mathbf{k} - \mathbf{k}_J)$$

NLL jet vertex and cone algorithm

$\mathbf{k}, \mathbf{k}'$ = Euclidian two dimensional vectors

$$\mathcal{S}_J^{(3,\text{cone})}(\mathbf{k}', \mathbf{k}-\mathbf{k}', xz; x) =$$

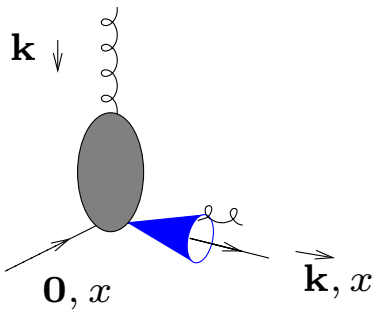

$$\mathcal{S}_J^{(2)}(\mathbf{k}, x)\,\Theta\left(\left[\frac{|\mathbf{k}-\mathbf{k}'|+|\mathbf{k}'|}{\max(|\mathbf{k}-\mathbf{k}'|,|\mathbf{k}'|)}R_{\text{cone}}\right]^2 - \left[\Delta y^2+\Delta\phi^2\right]\right)$$

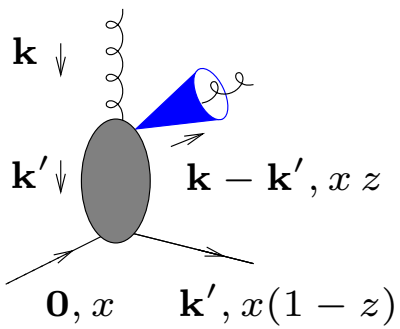

$$+\,\mathcal{S}_J^{(2)}(\mathbf{k}-\mathbf{k}', xz)\,\Theta\left(\left[\Delta y^2+\Delta\phi^2\right] - \left[\frac{|\mathbf{k}-\mathbf{k}'|+|\mathbf{k}'|}{\max(|\mathbf{k}-\mathbf{k}'|,|\mathbf{k}'|)}R_{\text{cone}}\right]^2\right)$$

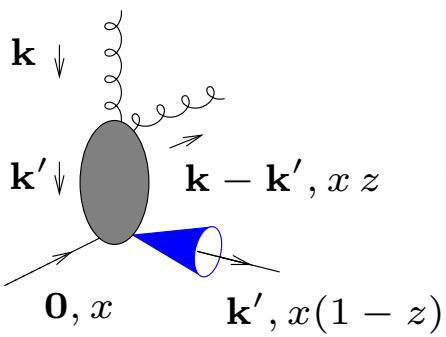

$$+\,\mathcal{S}_J^{(2)}(\mathbf{k}', x(1-z))\,\Theta\left(\left[\Delta y^2+\Delta\phi^2\right] - \left[\frac{|\mathbf{k}-\mathbf{k}'|+|\mathbf{k}'|}{\max(|\mathbf{k}-\mathbf{k}'|,|\mathbf{k}'|)}R_{\text{cone}}\right]^2\right),$$

Mueller-Navelet jets at NLL and finiteness

Using a IR safe jet algorithm, Mueller-Navelet jets at NLL are finite

- UV sector:
  - the NLL impact factor contains UV divergencies $1/\epsilon$
  - they are absorbed by the renormalization of the coupling: $\alpha_S \longrightarrow \alpha_S(\mu_R)$
- IR sector:
  - PDF have IR collinear singularities: pole $1/\epsilon$ at LO
  - these collinear singularities can be compensated by collinear singularities of the two jets vertices and the real part of the BFKL kernel
  - the remaining collinear singularities compensate exactly among themselves
  - soft singularities of the real and virtual BFKL kernel, and of the jets vertices compensates among themselves

This was shown for both quark and gluon initiated vertices (Bartels, Colferai, Vacca)

BFKL Green's function at NLL

NLL Green's function: rely on LL BFKL eigenfunctions

- NLL BFKLkernel is not conformal invariant
- LL $E_{n,\nu}$ are not anymore eigenfunction
- this can be overcome by considering the eigenvalue as an operator with a part containing $\frac{\partial}{\partial \nu}$
- it acts on the impact factor

$$\omega(n,\nu) = \bar{\alpha}_s \chi_0\left(|n|, \frac{1}{2}+i\nu\right) + \bar{\alpha}_s^2 \left[\chi_1\left(|n|, \frac{1}{2}+i\nu\right) - \frac{\pi b_0}{2N_c}\chi_0\left(|n|, \frac{1}{2}+i\nu\right)\underbrace{\left\{-2\ln\mu_R^2 - i\frac{\partial}{\partial\nu}\ln\frac{C_{n,\nu}(|\mathbf{k}_{J1}|, x_{J,1})}{C_{n,\nu}(|\mathbf{k}_{J2}|, x_{J,2})}\right\}}_{2\ln\frac{|\mathbf{k}_{J1}|\cdot|\mathbf{k}_{J2}|}{\mu_R^2}}\right],$$

LL substraction and s_0

- one sums up $\sum(\alpha_s \ln \hat{s}/s_0)^n + \alpha_s \sum(\alpha_s \ln \hat{s}/s_0)^n \quad (\hat{s} = x_1\, x_2\, s)$
- at LL s_0 is arbitrary
- natural choice: $s_0 = \sqrt{s_{0,1}\, s_{0,2}}$ $s_{0,i}$ for each of the scattering objects
  - possible choice: $s_{0,i} = (|\mathbf{k}_J| + |\mathbf{k}_J - \mathbf{k}|)^2$ (Bartels, Colferai, Vacca)
    - but depend on $\mathbf{k}$, which is integrated over
    - $\hat{s}$ is not an external scale ($x_{1,2}$ are integrated over)
  - we prefer

$$\left.\begin{aligned} s_{0,1} = (|\mathbf{k}_{J1}| + |\mathbf{k}_{J1} - \mathbf{k}_1|)^2 \;\to\; s'_{0,1} = \frac{x_1^2}{x_{J,1}^2}\mathbf{k}_{J1}^2 \\ s_{0,2} = (|\mathbf{k}_{J2}| + |\mathbf{k}_{J2} - \mathbf{k}_2|)^2 \;\to\; s'_{0,2} = \frac{x_2^2}{x_{J,2}^2}\mathbf{k}_{J2}^2 \end{aligned}\right\} \quad \frac{\hat{s}}{s_0} \;\to\; \frac{\hat{s}}{s'_0} = \frac{x_{J,1}\, x_{J_2}\, s}{|\mathbf{k}_{J1}|\,|\mathbf{k}_{J2}|} = e^{y_{J,1} - y_{J,2}} \equiv e^Y$$

- $s_0 \to s'_0$ affects
  - the BFKL NLL Green function
  - the impact factors:

$$\Phi_{\rm NLL}(\mathbf{k}_i; s'_{0,i}) = \Phi_{\rm NLL}(\mathbf{k}_i; s_{0,i}) + \int \mathrm{d}^2\mathbf{k}'\, \Phi_{\rm LL}(\mathbf{k}'_i)\, \mathcal{K}_{\rm LL}(\mathbf{k}'_i, \mathbf{k}_i) \frac{1}{2} \ln \frac{s'_{0,i}}{s_{0,i}} \qquad (1)$$

- numerical stabilities (non azimuthal averaging of LL substraction) improved with the choice $s_{0,i} = (\mathbf{k}_i - 2\mathbf{k}_{Ji})^2$
  (then replaced by $s'_{0,i}$ after numerical integration)
- (1) can be used to test $s_0 \to \lambda\, s_0$ dependence

Collinear improved Green's function at NLL

- one may improve the NLL BFKL kernel for $n = 0$ by imposing its compatibility with DGLAP in the collinear limit
  Salam; Ciafaloni, Colferai
- usual (anti)collinear poles in $\gamma = 1/2 + i\nu$ (resp. $1 - \gamma$) are shifted by $\omega/2$

- one practical implementation:
  - the new kernel $\bar{\alpha}_s \chi^{(1)}(\gamma, \omega)$ with shifted poles replaces

    $$\bar{\alpha}_s \chi_0(\gamma, 0) + \bar{\alpha}_s^2 \chi_1(\gamma, 0)$$

  - $\omega(0, \nu)$ is obtained by solving the implicit equation

    $$\omega(0, \nu) = \bar{\alpha}_s \chi^{(1)}(\gamma, \omega(0, \nu))$$

    for $\omega(n, \nu)$ numerically.
- there is no need for any jet vertex improvement because of the absence of γ and $1 - \gamma$ poles (numerical proof using Cauchy theorem "backward")
- this can be extended for all n

Motivation for asymmetric configurations

- Initial state radiation (unseen) produces divergencies if one touches the collinear singularity $\mathbf{q}^2 \to 0$

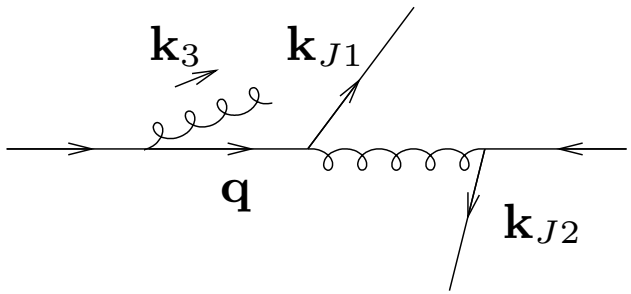

- they are compensated by virtual corrections
- this compensation is in practice difficult to implement, or *even incomplete*, when for some reason this additional emission is in a "corner" of the phase space (dip in the differential cross-section)
- this is the case when $\mathbf{k}_{J1} + \mathbf{k}_{J2} \to 0$
- this calls for a resummation of large remaing logs $\Rightarrow$ Sudakov resummation

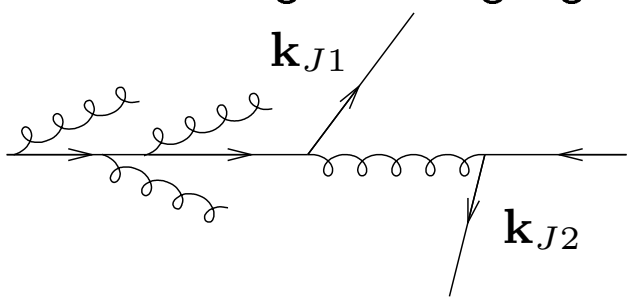

Motivation for asymmetric configurations

- since these resummation have never been investigated in this context, one should better avoid that region
- note that for BFKL, due to additional emission between the two jets, one may expect a less severe problem (at least a smearing in the dip region $|\mathbf{k}_{J1}| \sim |\mathbf{k}_{J2}|$)

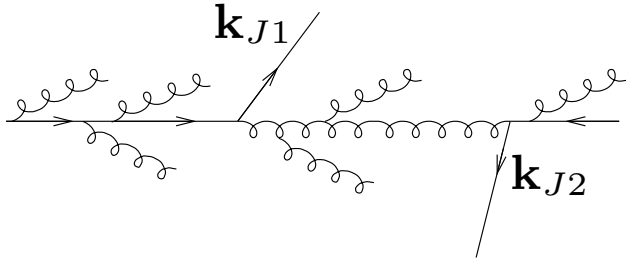

- this may however not mean that the region $|\mathbf{k}_{J1}| \sim |\mathbf{k}_{J2}|$ is perfectly trustable even in a BFKL type of treatment:
  in the limit $q_\perp^2 \equiv (\mathbf{k}_{J1} + \mathbf{k}_{J2})^2 \ll \tilde{P}_\perp^2 \equiv |\mathbf{k}_{J1}||\mathbf{k}_{J2}|$, at one-loop,

$$S_{qq\to qq} = -\frac{\alpha_s C_F}{2\pi} \ln^2 \frac{\tilde{P}_\perp^2 R_\perp^2}{c_0^2}$$

  where $R_\perp$ is the impact parameter, Fourier conjugated to $q_\perp$ ($c_0 = 2e^{-\gamma_E}$)
  $R_\perp \sim 1/q_\perp \Rightarrow$ suppression of this back-to-back configuration (on top of BFKL large Y effects) A. H. Mueller, L. Szymanowski, S. W., B.-W. Xiao, F. Yuan
- we thus think that a measurement in a region where both NLO fixed order and NLL BFKL are under control would be safer!

CMS measurement

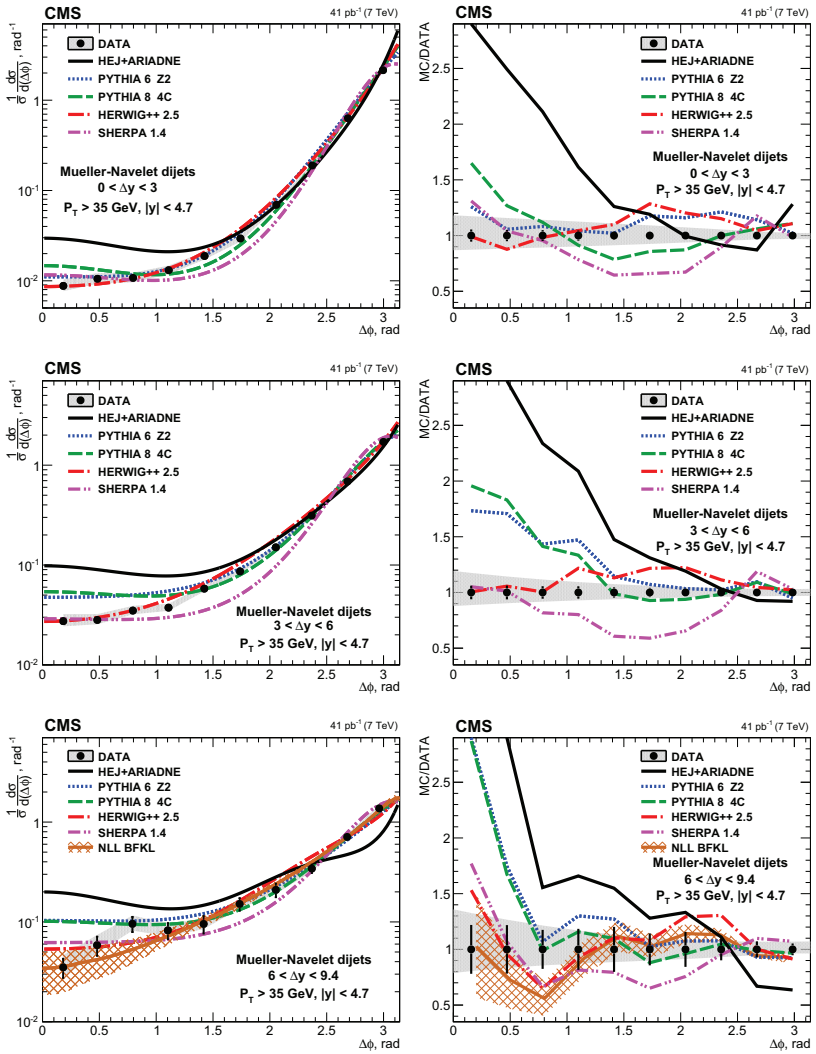

Figure 1: Left: Distributions of the azimuthal-angle difference, $\Delta\phi$, between MN jets in the rapidity intervals $\Delta y < 3.0$ (top row), $3.0 < \Delta y < 6.0$ (centre row), and $6.0 < \Delta y < 9.4$ (bottom row). Right: Ratios of predictions to the data in the corresponding rapidity intervals. The data (points) are plotted with experimental statistical (systematic) uncertainties indicated by the error bars (the shaded band), and compared to predictions from the LL DGLAP-based MC generators PYTHIA 6, PYTHIA 8, HERWIG++, and SHERPA, and to the LL BFKL-motivated MC generator HEJ with hadronisation performed with ARIADNE (solid line).

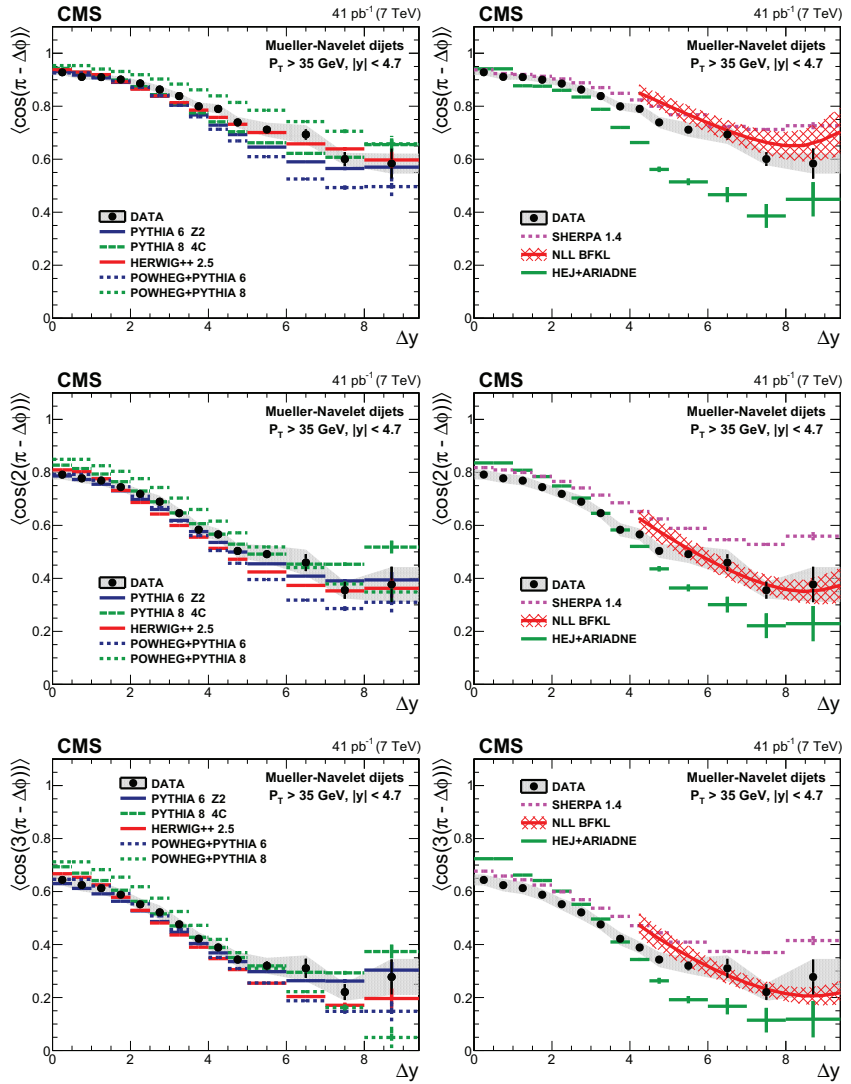

Figure 2: Left: Average $\langle\cos(n(\pi - \Delta\phi))\rangle (n = 1,2,3)$ as a function of Δy compared to LL DGLAP MC generators. In addition, the predictions of the NLO generator POWHEG interfaced with the LL DGLAP generators PYTHIA 6 and PYTHIA 8 are shown. Right: Comparison of the data to the MC generator SHERPA with parton matrix elements matched to a LL DGLAP parton shower, to the LL BFKL inspired generator HEJ with hadronisation by ARIADNE, and to analytical NLL BFKL calculations at the parton level ($4.0 < \Delta y < 9.4$).